JOC The Journal of Organic Chemistry

Article

pubs.acs.org/joc

Synthesis and Characterization of Binary-Complex Models of Ureas and 1,3-Dicarbonyl Compounds: Deeper Insights into Reaction Mechanisms Using Snap-Shot Structural Analysis

Takumi Azuma,[†] Yusuke Kobayashi,[†] Ken Sakata,[‡] Takahiro Sasamori,[§] Norihiro Tokitoh,[§] and Yoshiji Takemoto*[,†]

[†]Graduate School of Pharmaceutical Sciences, Kyoto University, Yoshida, Sakyo-ku, Kyoto 606-8501, Japan

[‡]Faculty of Pharmaceutical Sciences, Hoshi University, Ebara, Shinagawa-ku, Tokyo 142-8501, Japan

[§]Institute for Chemical Research, Kyoto University, Uji, Kyoto 611-0011, Japan

Supporting Information

ABSTRACT: The mechanism of the enantioselective Mannich reaction catalyzed by a hydrogen-bond (HB)-donor bifunctional organocatalyst has been fully investigated using experimental evidence and computational analysis. Several binary complexes have been designed as models of a catalyst and a nucleophile, where the urea moieties were linked to a 1,3-dicarbonyl compound through the diphenylacetylene motif. X-ray analysis of models **9** and **10** showed that the two N−H protons of the ureas interacted with the same carbonyl group via a double HB interaction. Further investigation of the crystallographic structure of **11** allowed for the direct observation of the labile ammonium−enolate intermediate formed between a bifunctional amino urea and 1,3-diketone. The *β*-keto ester−amino urea complex **12** reacted with several electrophiles at a remarkably fast rate to provide the corresponding adducts **15** and **17** as single diastereomers in excellent yields, respectively. A density functional theory calculation disclosed the details of the deprotonation and C−C bond-forming steps of the enantioselective Mannich reaction. The deprotonation of the 1,3-dicarbonyl moiety occurred predominantly via the enol form to give the ammonium−-enolate intermediate. These results should provide a deeper and more accurate understanding of the functional roles of the HB-donor and Brønsted base moieties of the catalyst.

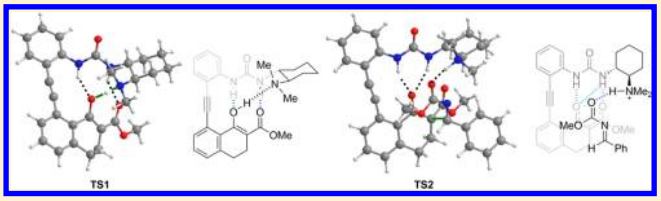

INTRODUCTION

Enzymes often use interdigitated hydrogen-bonding networks to promote specific reactions under mild conditions.[1] During the past decade, a growing number of organocatalytic systems have been developed by chemists as artificial small molecule systems that are capable of mimicking enzymes,[1d] and these systems have attracted considerable interest from synthetic organic chemists because of their ease-of-handling, low level of toxicity, and low cost.[2] The mechanisms of many different organocatalyzed reactions have also been explored using computational analyses[3] because a thorough understanding of these reaction mechanisms could lead to improvements in their catalytic activities as well as help to provide a deeper understanding of enzyme-catalyzed biological phenomena.

Urea and thiourea catalysts are representative of a group of organocatalysts that activate Lewis basic substrates through the formation of two hydrogen bonds.[4] In 2003, we reported that bifunctional thiourea catalysts[5] bearing H-bond donors and Lewis base functionalities promoted the Michael addition of 1,3-dicarbonyl compounds to nitroalkenes to give the Michael adducts in good yields and high enantioselectivities.[5a] Following from this work, an increasing number of asymmetric reactions catalyzed by a variety of HB-donor bifunctional organocatalysts have been developed.[6,7] The cooperative activation of the nucleophile and the electrophile by the tertiary amine and HB-donor moieties of these catalysts has been proposed to account for the significant enhancement in the rate and stereoselectivity of these reactions (ternary complex A in Figure 1).[5a]

Several theoretical studies were subsequently conducted on the bifunctionality of chiral thiourea-based organocatalysts,[8] which resulted in a slightly different mode of activation being proposed. According to this proposal, the nucleophile was sequentially activated by the thiourea and the tertiary amine, with the electrophile being activated by the resulting ammonium proton[8d] (ternary complex B in Figure 1). Although this new mechanism, which was based on a DFT calculation, was more promising than the original one, none of the proposed intermediates have been identified experimentally. For this reason, the details of this reaction mechanism remain unknown, even though a better understanding of this mechanism could be critical for the development of improved innovative catalytic asymmetric reactions. In sharp contrast to primary and secondary amine organocatalysts, which activate substrates via the formation of covalent bonds,[9] the intermediates formed during thiourea-catalyzed reactions cannot be detected spectroscopically because of the small

Received: January 7, 2014
Published: January 22, 2014

   dx.doi.org/10.1021/jo4028775 | J. Org. Chem. 2014, 79, 1805−1817

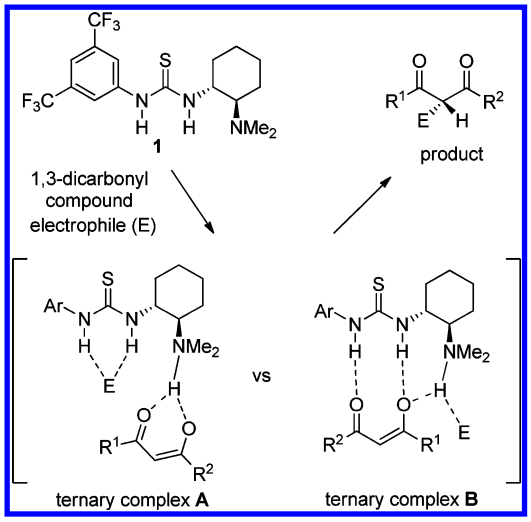

Figure 1. Proposed mechanism of the bifunctional thiourea-catalyzed reaction.

association constants resulting from the formation of binary complexes between the catalyst and the substrate (complex **C** in Figure 2). It would therefore be difficult to verify the existence of the reactive enol and/or enolate intermediates[10] predicted by computational analysis. Furthermore, it would not be possible to clearly establish the roles of individual active sites in the catalytic processes.

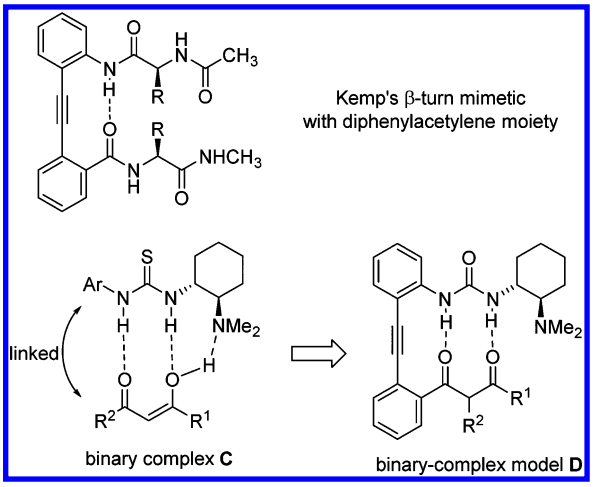

Figure 2. Conformationally rigid binary-complex models **D** with a diphenylacetylene motif.

To overcome this inevitable challenge, we planned to synthesize thermodynamically stable binary complexes that could mimic the intermediate formed between the catalyst and nucleophile via ternary complex B and evaluate their structural by spectroscopic properties. It was envisaged that a properly constructed motif would enable the direct observation of the labile reaction species.[11] With this in mind, the diphenylacetylene unit was selected as an ideal covalent linker for the thiourea and 1,3-dicarbonyl compounds (complex model **D** in Figure 2) because the 2-amino-2′-carboxyldiphenylacetylenes, which were developed by Kemp, are known to function as β-turn motifs in artificial β-sheet structures,[12] and it was envisaged that two fragments linked by this unit would form the appropriate intramolecular hydrogen bonding interactions between the carbonyl oxygen(s) and the N–H proton(s).[13] In this study, we describe the synthesis of four binary complex models **9**–**12** (Scheme 1) bearing the β-turn motif and the subsequent determination of their three-dimensional structures by ^{1}H NMR and X-ray crystallographic analyses to elucidate the intramolecular interactions between the thiourea moiety and 1,3-dicarbonyl fragment. Finally, the Mannich reaction between the *N*-Boc-imine and binary-complex model **12** was investigated to identify the absolute configuration and stereoselectivity of the products. In addition, DFT calculations were used to clarify the mechanistic details of the Mannich reaction and rationalize the experimental results.

Scheme 1. Synthesis of the Binary-Complex Models

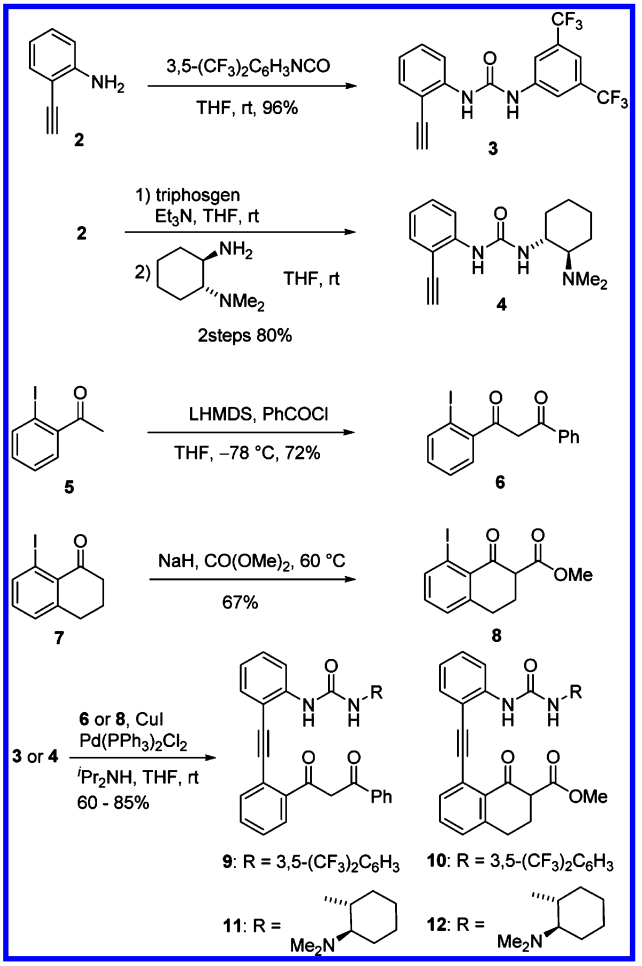

RESULTS AND DISCUSSION

Synthesis of the Diphenylacetylene-Linked Ureas and Aminoureas. We designed four binary-complex models **9**–**12** (Scheme 1) bearing a diphenylacetylene core that was capable of forming a β-turn conformation with an intramolecular N_{donor}–$O_{acceptor}$ hydrogen-bonding interaction. A urea was used as the hydrogen bond donor group instead of a thiourea because the high reactivity of thioureas can cause problems during the synthesis of target molecules.[14] Furthermore, to develop a deeper understanding of the effect of the bifunctionality of the catalysts, both the *N*-(2-dimethylaminocyclohexyl)urea and *N*-arylurea were incorporated in the binary-complex models. In contrast, the 1,3-diketone and β-keto ester were linked to the other side of the diphenylacetylene core as hydrogen bond acceptors. The synthesis of these

dx.doi.org/10.1021/jo4028775 | J. Org. Chem. 2014, 79, 1805–1817

models is shown in Scheme 1. Two different types of the upper fragment **3** and **4** were prepared from 2-ethynylaniline (**2**). The reaction of **2** with arylisocyanate provided the corresponding urea **3** in high yield. The amino urea **4** was obtained by the sequential treatment of **2** with triphosgene and *N*,*N*-dimethylcyclohexyl-1,2-diamine. The iodoketones **5** and **7** were acylated under basic conditions for the synthesis of the lower parts of the hydrogen-bond acceptors, and gave the corresponding diketone **6** and keto ester **8** products in good yields, respectively. We then proceeded to investigate the coupling of the upper and lower parts. The Sonogashira coupling[15] reactions of alkyne **3** with aryl iodides **6** and **8** proceeded smoothly in the presence of $Pd(PPh_3)_2Cl_2$ and CuI to afford the desired products **9** and **10** in 83 and 60% yields. The binary-complex models **11** and **12** of the bifunctional urea catalyst were synthesized by the coupling reactions of alkyne **4** with the aryl iodides **6** and **8**, respectively, in 75 and 85% yields under the same reaction conditions. Unfortunately, all of our attempts to prepare the corresponding thiourea adducts using a variety of different conditions were unsuccessful.

Structural Analysis of the Binary-Complex Analogues by NMR and X-ray Crystallography. Having successfully synthesized four of the desired models, we proceeded to investigate the ^{1}H NMR of compound **9** to determine whether this compound would readily form intramolecular hydrogen bonds between its diketone and urea moieties. The ^{1}H NMR spectra of **3**, a 1:1 mixture of **3** and **6**, and binary-complex model **9** are shown in Figure 3. Although the spectrum of diaryl

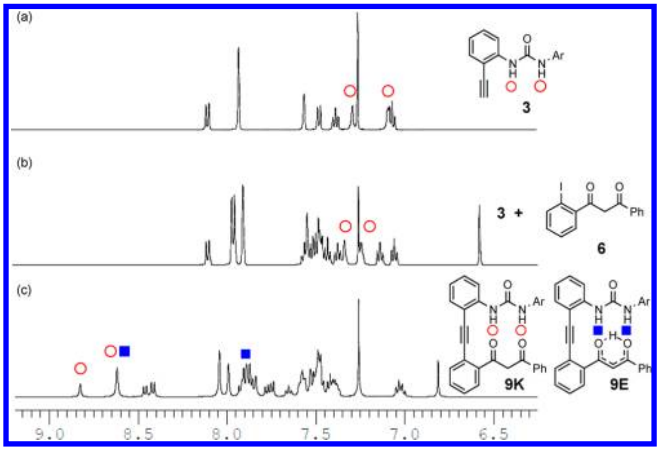

Figure 3. Partial ^{1}H NMR spectra (20 mM in $CDCl_3$) of (a) **3**, (b) a 1:1 mixture of **3** and **6**, and (c) **9**.

urea **3** contained two NH peaks at 7.08 and 7.28 ppm (Figure 3 (a), 20 mM in $CDCl_3$, rt), these NH peaks were shifted slightly downfield to 7.24 and 7.33 ppm when **3** was mixed with diketone **6** in a 1:1 ratio (Figure 3 (b)). In contrast, the NMR spectrum of **9** contained four NH signals, because the diketone moiety of **9** existed in both its keto and enol forms. Thus, the NH peaks were at 8.62 and 8.82 ppm in the keto form and 7.80–8.00[16] and 8.62 ppm in the enol form (Figure 3 (c)). In any event, these downfield shifts of the NH signals strongly suggest that the two NH protons of the urea were hydrogen bonded to the carbonyl group of the diketone. In addition, because the chemical shifts of the NH protons of **9** did not change even under highly dilute conditions (1.25 mM), which was distinct from the cases of **3**, an internal hydrogen bond would still be formed. It is noteworthy that the hydrogen-bonded complex **9** existed in both its keto and enol forms **9K** and **9E** in a ratio of 45:55, whereas the non-hydrogen-bonded 1,3-diketone **6** existed almost exclusively in its enol form (1:99). These results indicated that the internal hydrogen bond between the diketone and the urea was favored to such an extent that the six-membered hydrogen-bonding interaction of the 1,3-diketone moiety was dissociated.

To gain deeper insight into the structure of **9**, we grew good quality crystals of **9** for X-ray crystallographic analysis. The results of the X-ray analysis revealed that the crystals of **9** consisted of the keto form **9K**, as shown in Figure 4. We

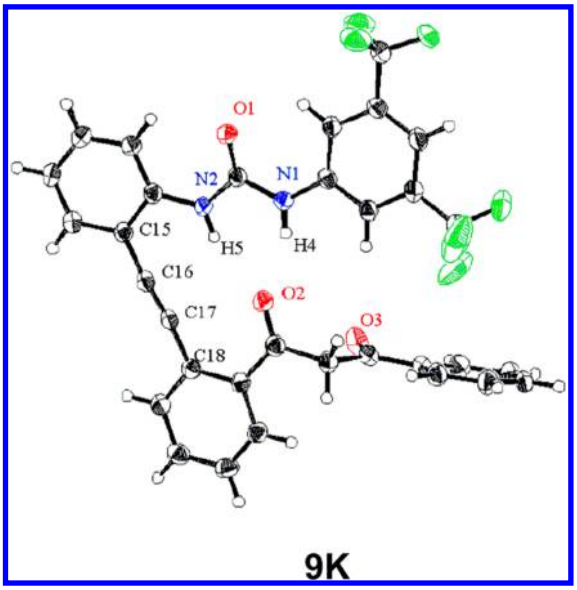

Figure 4. X-ray structure of **9K**. Selected bond length and angles: O(2)–H(4) 2.11 Å; O(2)–H(5) 2.14 Å; C(15)–C(16)–C(17) 173°; C(16)–C(17)–C(18) 172°.

anticipated that each NH proton of the urea would form an independent hydrogen bond with each carbonyl oxygen atom of the diketone (complex model **D** in Figure 2). Surprisingly, however, both NH protons of the urea only interacted with the proximal carbonyl oxygen of the diketone via a bifurcated hydrogen bond (NH···O = 2.14 and 2.11 Å), and the remaining carbonyl group was situated orthogonal to the hydrogen-bonded ketone and did not interact with any of the other functionalities. The bond angles of the two sp carbons were 172 and 173°, indicating that the linker between the two aryl groups had bent slightly to maintain the required thermodynamically stable conformation. This experimental observation implied that the alkyne moiety was flexible enough to preserve a favorable interaction[17] and confirmed that these models were suitable for further investigation.

Although the enol form **9E** predominated slightly over the keto form **9K** in a $CDCl_3$ solution, our efforts to prepare good-quality crystals of **9E** for X-ray analysis were unsuccessful. We then turned our attention toward using DFT calculations for **9E** and **9K** with B3LYP/6-31G* to identify the thermodynamically stable three-dimensional structures of these compounds as well as their most stable forms. The X-ray crystallographic structure of **9K** was directly used as the initial structure for the DFT calculation of **9K**. In contrast, the virtual structure of **9E** was constructed on the basis of the structure of **9K** and optimized using B3LYP/6-31G*. As a result, the keto form **9K** was predicted to be 0.8 kcal/mol less stable than the enol form **9E**.

dx.doi.org/10.1021/jo4028775 | J. Org. Chem. 2014, 79, 1805–1817

The most thermodynamically stable structure of **9E** is depicted in Figure 5. The calculated NH···O distances were 2.01 and

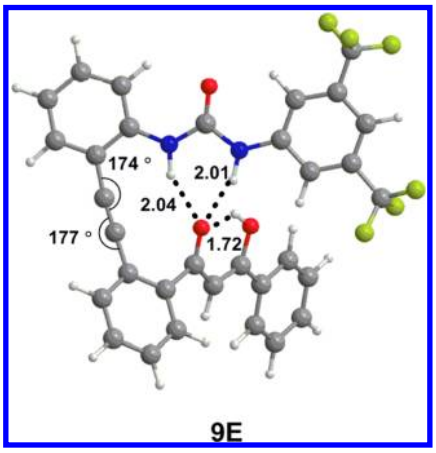

Figure 5. Estimated structure of **9E** from the DFT calculation.

2.04 Å and, therefore, much shorter than the values observed for **9k** in the solid state. The OH···O distance (internal hydrogen bond) was 1.72 Å.

We then examined the chemical structure of amino urea **11** by NMR and X-ray analysis. The ^{1}H NMR spectra of **4**, a 1:1 mixture of **4** and **6**, and the binary-complex model **11** are shown in Figure 6. In a similar manner to **9**, the NH protons of

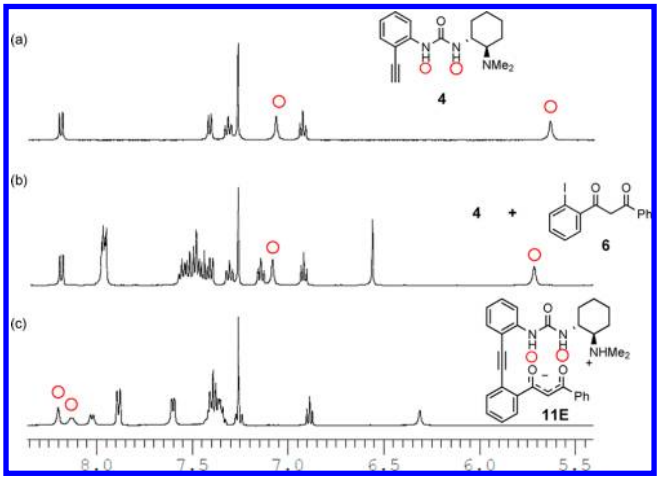

Figure 6. Partial ^{1}H NMR spectra (20 mM in $CDCl_3$) of (a) **4**, (b) a 1:1 mixture of **4** and **6**, and (c) **11**.

11 were shifted downfield in comparison to those of **4**, which confirmed the existence of an internal hydrogen bonding interaction between the urea and the diketone (Figure 6, (a) vs (c)). The ratio of the keto form **11K** to the enol form **11E**, however, did not change in a similar manner to that observed for compound **6** and retained the same value (**11K**:**11E** = <1:>99). The X-ray structure of **11** clearly demonstrated that ammonium enolate **11E** was generated by the reaction of the 1,3-diketone with the dimethylamino group and that both of the oxygen atoms (i.e., C═O(2) and C═O(3)) of the resulting enolate anion formed double hydrogen bonds with an ammonium proton and either an N(2)H(18) or N(3)H(19) proton. The precise positions of the two NH protons and the ammonium proton were estimated by the DFT calculation on the basis of the X-ray structure of **11E** (Figure 7).[18] By

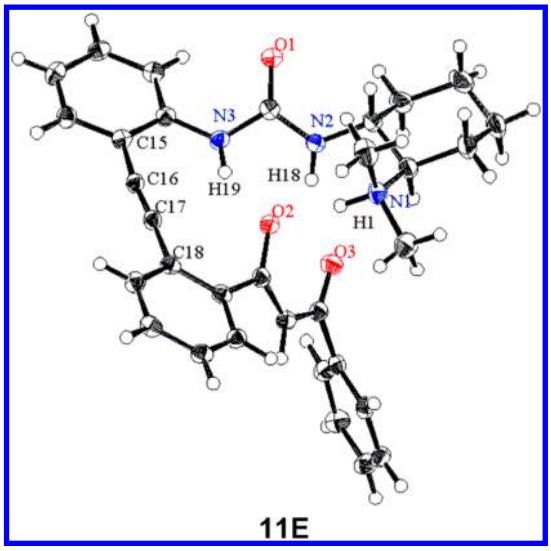

Figure 7. X-ray structure of **11E**. Selected bond length: O(2)–H(19) 2.04 Å; O(3)–H(18) 2.07 Å; O(2)–H(1) 1.74 Å; O(3)–H(1) 2.49 Å.

introducing the tertiary amine to the catalyst, the acidic proton of the 1,3-diketone was completely deprotonated to afford a thermodynamically stable enolate anion. This rationale reasonably explains the distinct behavior of the binary-complex models **9** and **11** in terms of the ratios of the keto and enol forms. Surprisingly, however, the interaction between the ammonium proton and the carbonyl oxygen C═O(2) proximal to alkyne was stronger than the interaction with the distal carbonyl oxygen C═O(3). The distances between the ammonium proton and the carbonyl oxygens O(2) and O(3) were 1.74 and 2.49 Å.

We then proceeded to investigate the cyclic β-keto ester derivatives **10** and **12** bearing less acidic protons to clarify their structures and properties compared with those of the acyclic diketones **9** and **11**. The ^{1}H NMR spectra of **3**, a 1:1 mixture of **3** and **8**, and **10** are shown in Figure 8, whereas the ^{1}H NMR spectra of **4**, a 1:1 mixture of **4** and **8**, and **12** are shown in Figure 9. A comparison of these spectra strongly indicated that the β-turn mimetics **10** and **12** possessed an internal hydrogen bond between their urea NH protons and one of the carbonyl groups of their keto esters. In addition, only the keto form (>99%) was detected in the ^{1}H NMR spectra of **10** and **12**,

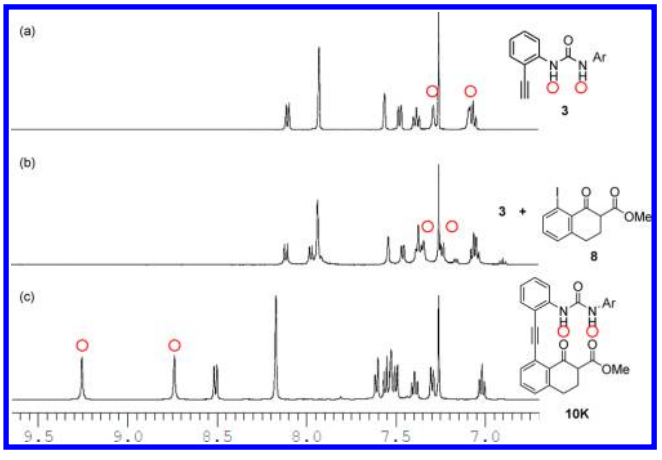

Figure 8. Partial ^{1}H NMR spectra (20 mM in $CDCl_3$) of (a) **3**, (b) a 1:1 mixture of **3** and **8**, and (c) **10**.

dx.doi.org/10.1021/jo4028775 | J. Org. Chem. 2014, 79, 1805–1817

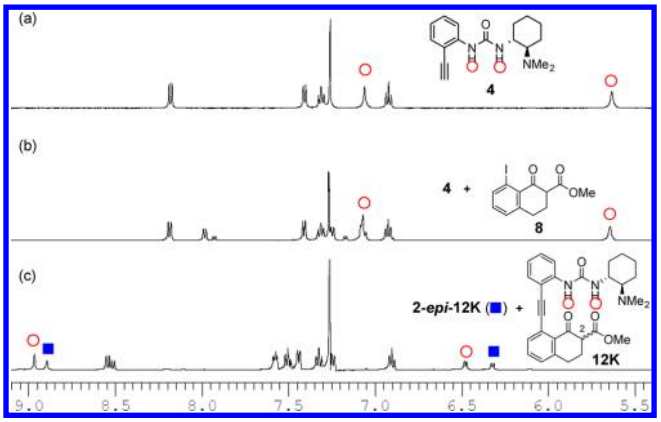

Figure 9. Partial ^{1}H NMR spectra (20 mM in $CDCl_3$) of (a) **4**, (b) a 1:1 mixture of **4** and **8**, and (c) **12**.

whereas the non-hydrogen-bonded β-keto ester **8** existed as an 80:20 mixture of its keto and enol forms in solution. Furthermore, these results were consistent with the trends observed for compounds **6** and **9**. The ^{1}H NMR spectrum of amino urea **12** contained a pair of signals because of the existence of two diastereomers resulting from the chirality of the β-keto ester moiety. Because β-keto ester **12** possessed a less acidic proton than diketone **11**, the equilibrium for the deprotonation reaction of **12** by the internal amine was biased toward **12K**, and it was therefore not possible to detect the enolate form by ^{1}H NMR.

We succeeded in growing good-quality crystals of **10**, and the X-ray crystal structure of this urea–keto ester complex is shown in Figure 10. In a manner similar to that of compound **9**, the X-ray structure of **10** revealed that the two NH protons of the urea only interacted with the carbonyl oxygen of the ketone via a bifurcated hydrogen bond. In contrast, the ester group of **10** was oriented perpendicularly to the hydrogen-bonded ketone. Although we were unable to prepare good quality crystals of **12** for X-ray analysis, we feel it would be reasonable to consider that the amino urea model **12** would adopt the keto form similar to urea **10** based on the similarities between their ^{1}H NMR spectra. The detailed reaction mechanism of **12** using DFT calculation will be discussed below.

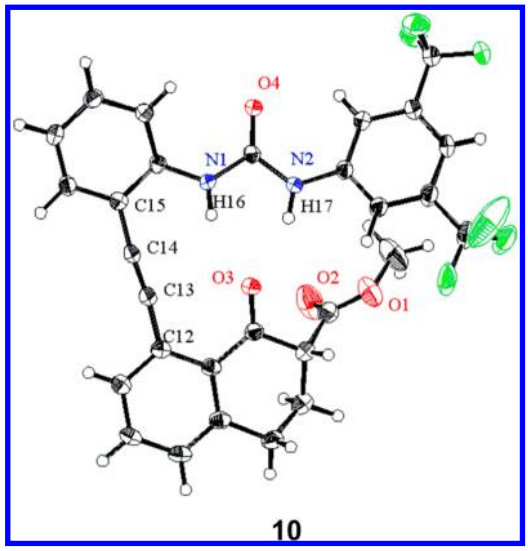

Figure 10. X-ray structure of **10**. Selected bond length and angles: O(3)–H(16) 2.17 Å; O(3)–H(17) 2.08 Å; C(12)–C(13)–C(14) 173°; C(13)–C(14) –C(15) 174°.

Nucleophilic Reactions of Binary-Complex Models 11 and 12 with Several Electrophiles. Having identified the precise 3D structures of the binary-complex models **11** and **12**, we proceeded to investigate their reactions with several electrophiles to determine whether these reactions would proceed in the same way as the corresponding and previously reported catalytic reactions (Scheme 2).[5a,e,h]

Scheme 2. Nucleophilic Reactions of the Binary-Complex Models 11 and 12

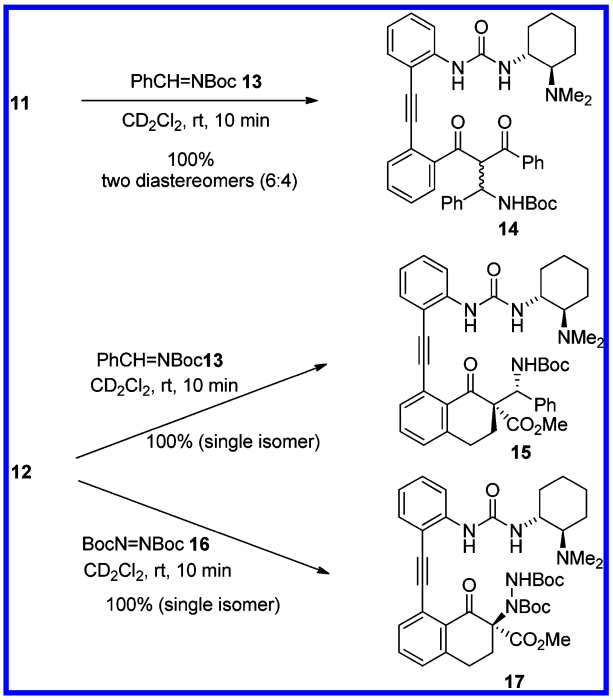

Disappointingly, the reaction of **11** with β-nitrostyrene gave a complex mixture due to the instability of the products. However, the same compound **11** underwent a Mannich reaction with *N*-Boc-imine **13** to give the desired product as a diastereomeric mixture (ca. 6:4), presumably because of the epimerization of the 1,3-dicarbonyl moiety.[5h] We then changed the substrate from diketone **11** to keto ester **12**, which would provide a chiral quaternary carbon center. In contrast to **11**, the Mannich reaction of **12** with *N*-Boc-imine **13** was complete within 10 min and proceeded stereoselectively to give the addition product **15** as a single isomer. The hydrazine derivative **17** was also synthesized as a single product via the simple treatment of **12** with di-*tert*-butyl azodicarboxylate **16** in CD_2Cl_2 at room temperature. It should be mentioned that this reaction proceeded quickly with an unprecedented level of stereoselectively, demonstrating that amino urea moiety functioned efficiently to activate the electrophiles and nucleophiles. The absolute configuration of **17** was determined by the chemical transformation of **8** into **17** and **20** via a catalytic asymmetric hydrazination reaction in the presence of bifunctional catalyst, followed by a Sonogashira coupling reaction with amino urea **4** (Scheme 3). According to our previous report, we then performed the aminobenzothiadiazine[7d] (**18**)-catalyzed reaction of **8** with **16**,[5e,19] and the desired adduct **19** was obtained in 97% yield, albeit with 53% ee.[20] The absolute configuration of **19** was elucidated to be *S* by

dx.doi.org/10.1021/jo4028775 | J. Org. Chem. 2014, 79, 1805–1817

Scheme 3. Determination of the Absolute Configuration of 17

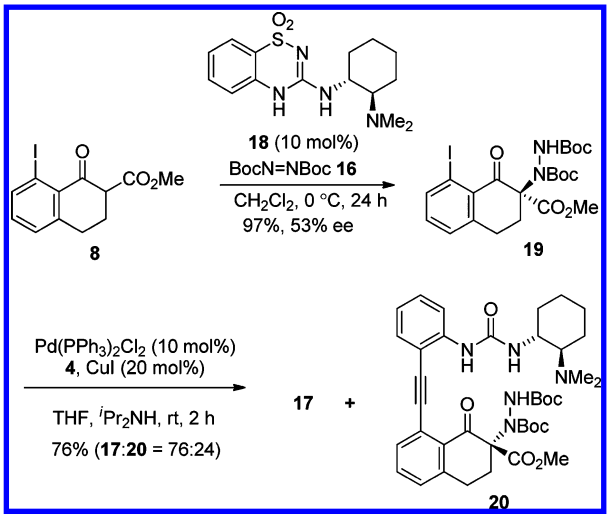

Scheme 4. Determination of the Absolute Configuration of 15

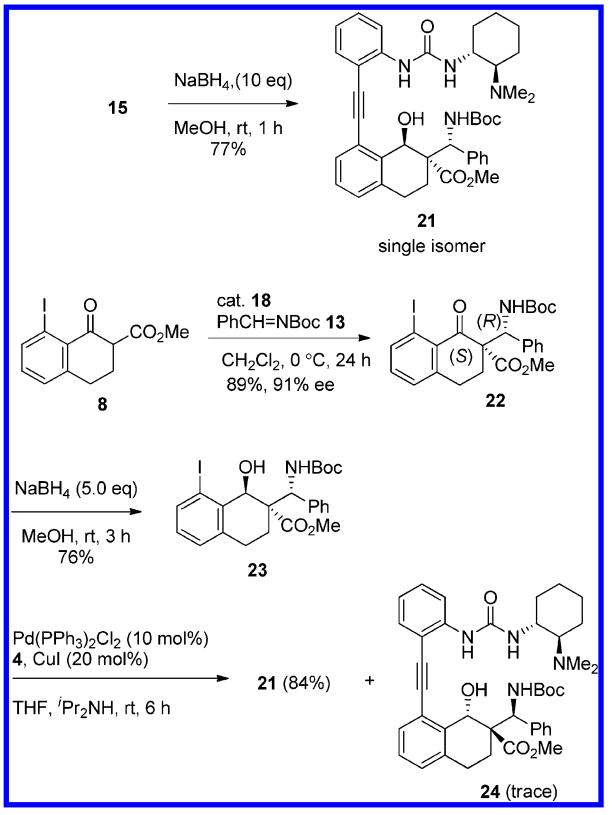

comparison with a previous report.[5e] The subsequent reaction of **19** with amino urea **4** gave the coupling products **17** and **20** as a mixture of diastereomers (76:24).[21] By comparing their ^{1}H NMR spectrum of this mixture with that of the diastereomerically pure product **17** derived from **12**, the major product prepared from **19** was revealed to be **17**, from which the absolute configuration of **17** was unambiguously determined to be *S*. These experimental results indicated that the aminourea moieties of **11** and **12** functioned in a similar manner to the original catalyst, such as **1** and **18**. Furthermore, these results demonstrated that these biaryl compounds were suitable models for the elucidation of the detailed reaction mechanisms.

Finally, we attempted to determine the absolute configuration of **15** in the same manner (Scheme 4), but the transformation of **8** into **15** was unsuccessful because the retro-Mannich reaction of **15** proceeded under the Sonogashira coupling reaction conditions.[15] Therefore, we prepared alcohol **21** by the reduction of **15** with $NaBH_4$. The reduction proceeded diastereoselectively to give the desired monoalcohol **21** as the single isomer. The same alcohol **21** was also synthesized via an alternative route involving the catalytic asymmetric Mannich reaction. The asymmetric Mannich reaction with **8** provided the desired adduct **22** in 89% yield and 91% ee.[22] The absolute configuration of **22** was elucidated to be (2*S*,1′*R*) based on the previous report.[5h] The reduction of **22** with $NaBH_4$ followed by the coupling reaction of the resultant adduct **23** with **4** gave the target molecule **21**. The reaction of **23** with **4** gave the coupling product **21** in 84% yield together with a trace amount of **24**.[23] By comparing their ^{1}H NMR spectra with that of **21** derived from **12**, the major product prepared from **23** (er = 95.5:4.5) was revealed to be **21**, from which the absolute configuration of **15** was unambiguously determined.

Theoretical Studies on Mannich Reaction of Binary-Complex Models 12 Based on a Snapshot X-ray Analysis. The reactions of **12** with several different electrophiles were revealed to proceed very rapidly and in a highly stereoselective manner. Furthermore, a detailed 3D structure of the binary-complex model **11**, which would be a hypothetical reaction intermediate in the corresponding catalytic reactions, was first clarified by X-ray crystallographic analysis. Based on these results, we conducted a theoretical study of the Mannich reaction of **12** with *N*-methoxycarbonylimine. All of the theoretical optimizations were performed using Gaussian 09[24] at the B3LYP/6-31G* level.[25] Once the stationary points were obtained at the B3LYP/6-31G* level, the harmonic vibrational frequencies were calculated at the same level to estimate the Gibbs free energy. All of the Gibbs free energy values reported in this paper were calculated for a temperature of 298.15 K. All of the transition structures reported were optimized without constraints and the intrinsic reaction coordinate (IRC) routes were calculated in both directions toward the corresponding minima for each transition-state structure. The IRC calculations failed to reach the energy minima on the potential energy surface for some of the transition states and, in those cases, we therefore carried out geometry optimizations as a continuation of the IRC path. Since we could not prepare good quality crystals of **12** for X-ray analysis, the most stable 3D structures of both the keto and enol forms of **12** were estimated using DFT calculations. The ^{1}H NMR studies of **12** strongly suggested that the binary-complex model **12** existed in the keto forms **12K-1** and **12K-2** (an epimer of **12K-1**) in solution, but the virtual structure of the enol form **12E** was also optimized. The resulting three conformations **12K-1**, **12K-2**, and **12E** are shown in Figure 11. From the estimated Gibbs free energies of these three conformers, the enol form **12E** and the keto form **12K-2** were predicted to be 4.1 and 0.9 kcal/mol above the keto form **12K-1**. We then searched for the optimal structure of *N*-methoxycarbonylimine and found two conformations of the imine (**imine A** and **imine B**) (Figure 12). **Imine B** was determined to be more stable than **imine A** by 2.2 kcal/mol. The energy barrier for a conformational change was 3.3 kcal/mol, and the two conformations were therefore in equilibrium. Next, we searched the transition state **TS1** for the

dx.doi.org/10.1021/jo4028775 | J. Org. Chem. 2014, 79, 1805−1817

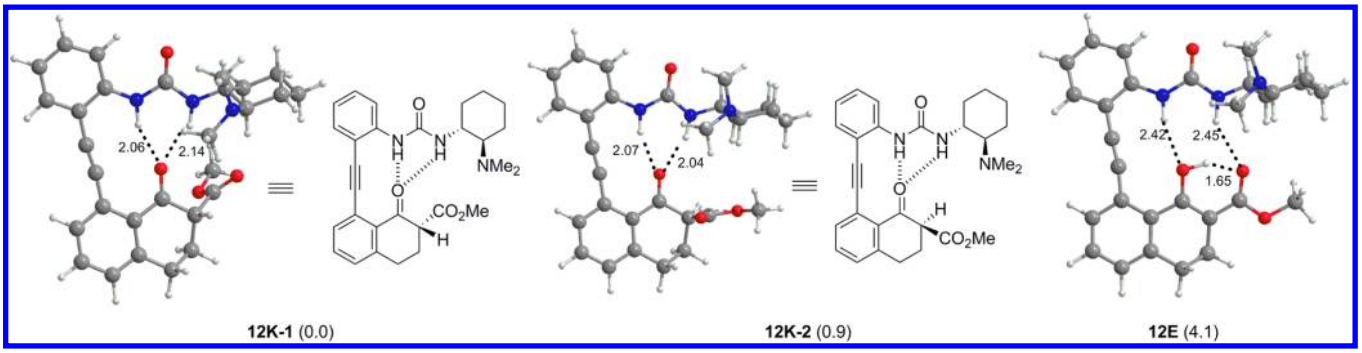

Figure 11. Optimized structures of **12**. Bond distances characteristic for H-bonds are given in angstroms. Relative Gibbs free energies (kcal/mol) are in parentheses.

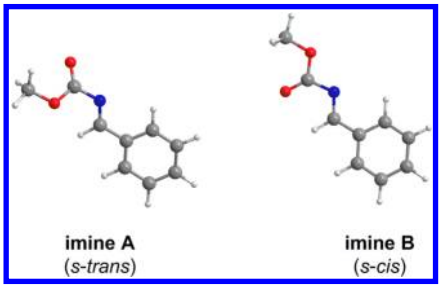

Figure 12. Optimized structure of the imine.

transformation of **12** into an ammonium enolate **IM1** like the binary complex **11** (Figure 13). Although the keto form **12K-1** was energetically more stable than the enol form **12E**, the ΔG (28.0) of **TS1K**, the transition state from **12K-1** (0.0) into **IM1** (8.3), was too large for the internal deprotonation from the keto ester moiety by the tertiary amine to occur at room temperature. In contrast, the generation of the enolate **IM1** from the enol form **12E** via **TS1E** appeared to be much more feasible than that from **12K-1**, judging from the energy difference between **12E** (4.1) and **TS1E** (8.1). Taking into account the good reactivity and high selectivity of the Mannich reaction of **12**, it would be reasonable to consider that the enol form **12E**, which existed only as a trace in solution, must play an important role in the formation of the ammonium enolate **IM1**, whereas **12E** could not be detected in the ^{1}H NMR.

Having elucidated the transition-state geometry for the enolate formation of **12**, as shown in Figure 13, we proceeded to explore the carbon−carbon bond formation reaction and found two channels for this reaction. According to one channel, the ammonium proton of **IM1** coordinated with **imine A** (channel A, Figure 14), whereas in the other channel, the ammonium proton of **IM1** coordinated with **imine B** (channel B, Figure 15). In the optimized geometry of the binary complex **IM2a**, the ammonium proton only coordinated strongly with the oxygen atom of the imine with a hydrogen bond distance of 1.79 Å. However, in the optimized geometry of the binary complex **IM2b**, the ammonium proton coordinated with both the oxygen and nitrogen atoms of the imine and the hydrogen bond distances were longer than that of **IM2a**. Although **imine A** was less stable than **imine B**, the binary complex **IM2a** (17.1) was more stable than **IM2b** (21.8). We then obtained the transition state geometries of the two channels ($\mathbf{TS}_{\mathbf{2a-3a}}$, $\mathbf{TS}_{\mathbf{2b-3b}}$) and found that the nature of the hydrogen bond between the ammonium proton and the imine remained unchanged mainly from **IM2**. In both of the transition states, we observed some weakening of the urea−ketoester interaction and the strengthening of the ammonium−imine interaction because of the occurrence of a charge transfer process from the anionic ketoester to the electron-deficient imine. The optimized structures of the intermediates following the C−C bond formation were also obtained. In both channels, the C−C bond formation reactions were predicted to be kinetically feasible processes with the transition state $\mathbf{TS}_{\mathbf{2a-3a}}$ lying 12.0 kcal/mol above **IM2a** or $\mathbf{TS}_{\mathbf{2b-3b}}$ lying 13.1 kcal/mol above **IM2b**. However, since $\mathbf{TS}_{\mathbf{2a-3a}}$ was predicted to be 5.8 kcal/mol lower in energy than $\mathbf{TS}_{\mathbf{2b-3b}}$, it was predicted that the C−C bond formation in the Mannich reaction would occur predominantly in channel A. The C−C bond formation was predicted to be the rate- and stereodetermining step, because this conversion step from **IM2** (17.1) to $\mathbf{TS}_{\mathbf{2a-3a}}$ (29.1) possessed the highest energy difference. Although the reaction proceeds via **IM3a** to give **TM** in channel A, there was no intermediate between $\mathbf{TS}_{\mathbf{2b-3b}}$ and **TM** in channel B. The significant stability of **TM** (9.8) was attributed to the double intramolecular hydrogen bonding interaction between MeOCONH and the CO_2Me (2.21 Å) and NMe_2 (2.71 Å) groups (Figure 15). Furthermore,

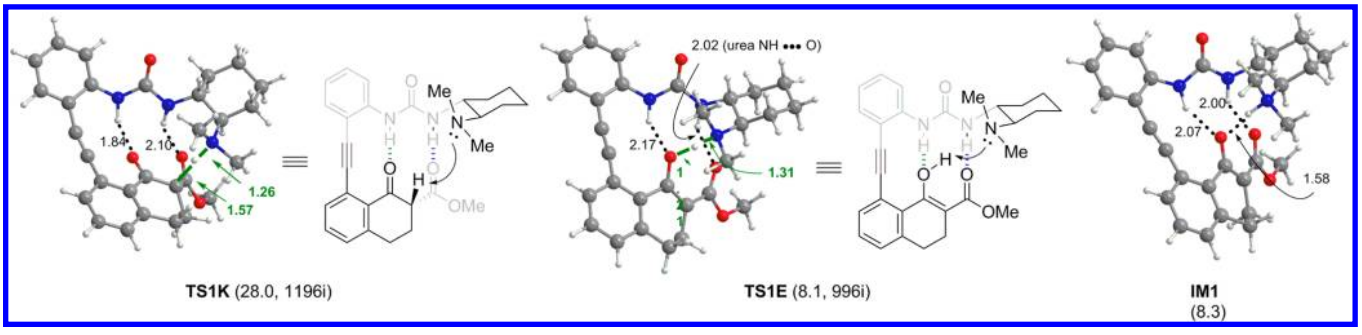

Figure 13. Optimized structures of **TS1K**, **TS1E**, and **IM1**.

dx.doi.org/10.1021/jo4028775 | J. Org. Chem. 2014, 79, 1805−1817

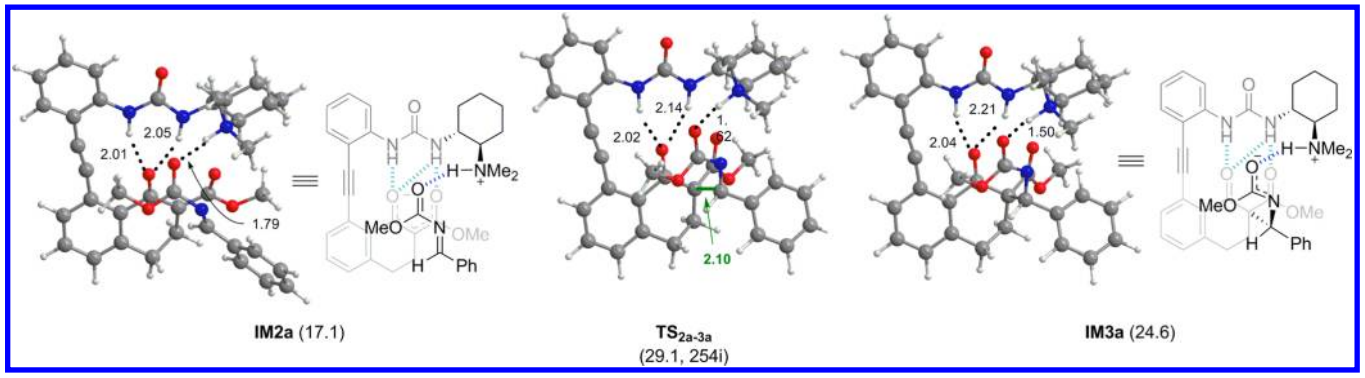

Figure 14. Optimized structures in channel A.

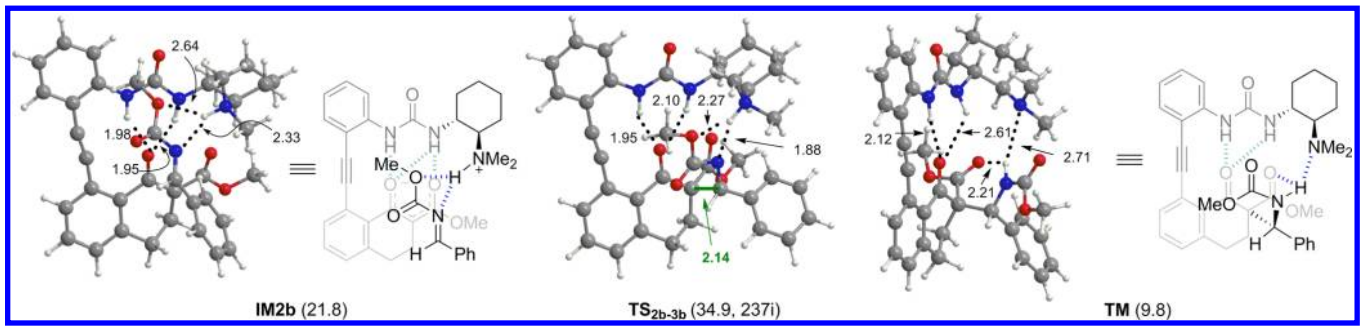

Figure 15. Optimized structures in channel B and TM.

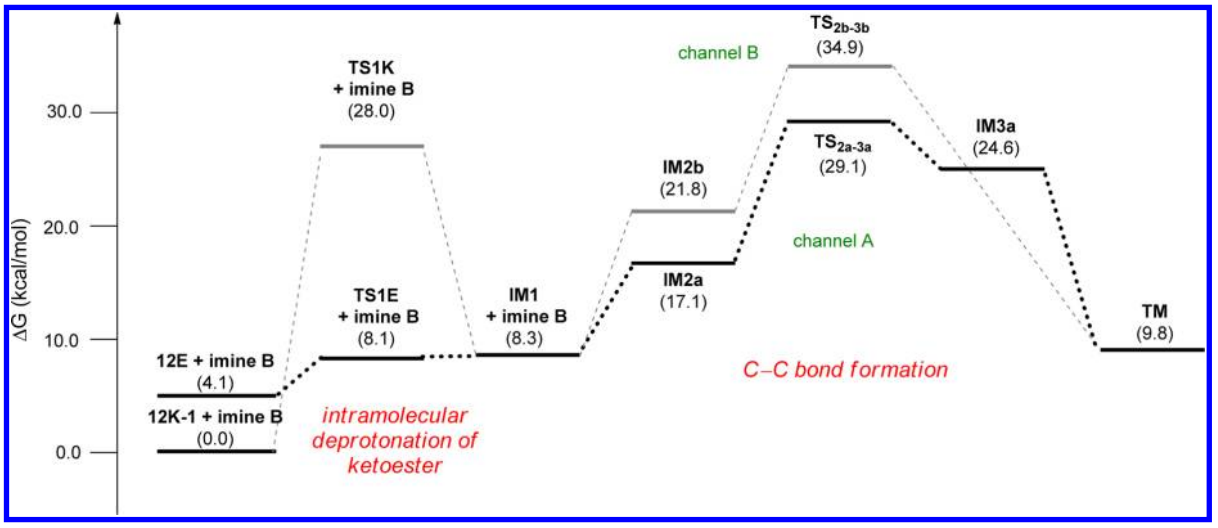

Figure 16. Energy profile of the Mannich reaction.

the two NH protons of the urea readily formed hydrogen bonds with the ketone via double hydrogen bonds in the **TM** (2.12 and 2.61 Å). These internal hydrogen bonds significantly stabilized the final product **18**, and effectively provided the driving force for the Mannich reaction. Furthermore, the energy profile of the Mannich reaction is shown in Figure 16.[26,27] Compared with the transition state affording the other diastereomer,[28] the activation energy for the C−C bond formation was greater than that of TS_{2a-2b} by 14.1 kcal. This calculations was consistent with the experimental result where the Mannich reaction only gave a single isomer **15**.

■ CONCLUSION

We have synthesized and presented the detailed structures of several urea−dicarbonyl complex models linked with diaryl alkynes by ^{1}H NMR and X-ray crystallography. The properly constituted models allowed for the direct observation of the labile and reactive intermediate, which would have been otherwise very difficult to detect. In the keto-forms of the binary complex models **9K** and **10**, only the ketone carbonyl oxygen proximal to the tether participated in the formation of intramolecular hydrogen bonding interaction with the two NH protons of the urea, leading to the formation of a bifurcated hydrogen bond. In contrast, the diketone complex **11** bearing an amine−urea moiety, formed an ammonium−enolate complex and existed in an ion pair, where a double-hydrogen-bonding interaction between each oxygen atom of the enolate and each NH proton of the urea was observed. We also confirmed that this ion pair of the binary complex model played a crucial role in the efficient and stereoselective reactions

dx.doi.org/10.1021/jo4028775 | J. Org. Chem. 2014, 79, 1805−1817

of this species with several electrophiles, in a manner very similar to that of the nonlinked bifunctional amino−(thio)urea catalysts.[4,5]

Based on the information obtained from our established binary-complex models, we conducted a computational investigation of the stereoselective Mannich reaction, and the main conclusions of the study can be summarized as follows: (i) the deprotonation of the methine proton of the 1,3-dicarbonyl moiety occurred predominantly via the enol form, even though almost all of the 1,3-dicarbonyl moiety existed in the keto form in solution; (ii) in the C−C bond-forming step, the conformation of the imine changed (from **imine B** to **imine A**) to afford a favorable transition state, where only the carbonyl oxygen atom of the imine interacted rigidly with the ammonium proton; and (iii) the ammonium enolate approached the imine exclusively from its *Re* face[28] to give the corresponding adduct as a single diastereomer.

These results strongly support the reaction mechanism via the ternary complex B (Figure 1) proposed by Pápai.[8d] As described in this paper, snapshot structural analysis using the appropriate reaction intermediate has been demonstrated as a powerful method to accurately elucidate the reaction mechanism. The application of this snapshot analysis of the other routes (ternary complex A, Figure 1) is currently underway[29] in our laboratory and will be reported in due course.

EXPERIMENTAL SECTION

General Information. All nonaqueous reactions were carried out under a positive atmosphere of argon in dried glassware unless otherwise noted. All the solvents and materials were obtained from commercial suppliers and used without further purification. Column chromatography was performed on silica gel (230−400 mesh) or silica gel (NH, 100−200 mesh), and flash column chromatography was performed on silica gel (spherical/40−100 μm). Reactions and chromatography fractions were analyzed using precoated silica gel plate. All melting points were measured on a melting point apparatus and are uncorrected. IR spectra were measured on FTIR. Unless otherwise noted, NMR spectra were obtained in $CDCl_3$. ^1H NMR (500 MHz) spectra were measured and chemical shifts are reported in δ (ppm) relative to TMS (in $CDCl_3$), which was used as an internal reference standard. ^{13}C NMR (126 MHz) spectra were also recorded and referenced to the residual $CHCl_3$ signal. ^1H NMR multiplicities are reported as follows: br = broad; m = multiplet; s = singlet; d = doublet; t = triplet; q = quartet; sep = septet. Low-resolution and high-resolution mass spectra were obtained using an LCMS-IT-TOF fitted with an ESI or FAB. Optical rotations were recorded on a polarimeter with a path length of 1 cm; concentrations are quoted in grams per 100 mL. $[\alpha]_D$ values were measured in 10^{-1} deg cm^2 g^{-1}. Enantiomeric excesses were determined by high-performance liquid chromatography (HPLC) analysis. Unless otherwise noted, all materials and solvents were purchased and used without purification. All noncommercially available substrates were prepared according to the literature procedure as indicated below.

*1-[3,5-Bis(trifluoromethyl)phenyl]-3-(2-ethynylphenyl)urea (**3**).* To a solution of **2**[30] (2.0 mmol, 234 mg) in THF (5.0 mL) was added 3,5-bis(trifluoromethyl)phenyl isocyanate (2.0 mmol, 510 mg). After being stirred at room temperature for 6 h, the mixture was concentrated in vacuo. The residue was purified by recrystallization (*n*-hexane/AcOEt) to afford **3** (707 mg, 95%): white solid; mp 197−198 °C; ^1H NMR (acetone-d_6) δ 9.45 (s, 1H), 8.31 (d, J = 7.8 Hz, 1H), 8.18 (s, 2H), 8.05 (s, 1H), 7.63 (s, 1H), 7.47 (d, J = 7.8 Hz, 1H), 7.40 (dd, J = 7.8, 7.8 Hz, 1H), 7.06 (dd, J = 7.8, 7.8 Hz, 1H), 4.13 (s, 1H) ppm; ^{13}C NMR (acetone-d_6) δ 152.7, 142.7, 141.4, 133.3, 132.51 (q, J_{C-F} = 33 Hz), 124.4 (q, J_{C-F} = 275 Hz), 130.7, 123.4, 120.2, 119.1, 115.9, 111.9, 86.4, 79.8 ppm; IR (ATR) 3313, 1657, 1555 cm^{-1}; MS (FAB) 373 (MH^+, 100); HRMS (ESI) calcd for $C_{17}H_{11}F_6N_2O$ (MH^+) 373.0770, found 373.0767.

*1-[(1R,2R)-2-(Dimethylamino)cyclohexyl]-3-(2-ethynylphenyl)-urea (**4**).* To a solution of triphosgen (2.2 mmol, 630 mg) in THF (10 mL) was added a solution of **2** (4.3 mmol, 500 mg) and NEt_3 (17 mmol, 1.72 g) in THF (10 mL) dropwise at 0 °C. After being stirred at room temperature for 1 h, the mixture was filtrated through a pad of Celite, and the filtrate was concentrated in vacuo to give the crude isocyanate, which was then dissolved in THF (10 mL). To this solution was added (1*R*,2*R*)-N^1,N^1-dimethylcyclohexane-1,2-diamine (505 mg, 3.6 mmol), and the resulting mixture was stirred at room temperature for 5 h. The mixture was then concentrated in vacuo to afford a crude product, which was purified by silica gel chromatography ($CHCl_3$/MeOH = 10:1) to give **4** (981 mg, 80%): white solid; mp 137−138 °C; $[\alpha]^{25}_D$ −17.8 (*c* 2.30, $CHCl_3$); ^1H NMR ($CDCl_3$) δ 8.18 (d, J = 7.7 Hz, 1H), 7.40 (d, J = 7.7 Hz, 1H), 7.29 (br, 1H), 7.29 (dd, J = 7.7, 7.7 Hz, 1H), 6.90 (dd, J = 7.7, 7.7 Hz, 1H), 6.09 (br, 1H), 3.51 (s, 1H) 3.50 (m, 1H), 2.46 (m, 2H), 2.32 (s, 6H), 1.83−1.90 (m, 2H), 1.69−1.70 (m, 1H), 1.15−1.36 (m, 4H) ppm; ^{13}C NMR ($CHCl_3$) δ 155.3, 141.2, 132.2, 130.1, 121.4, 118.4, 109.7, 83.8, 79.9, 66.3, 52.0, 39.9, 33.3, 25.3, 24.6, 21.1 ppm; IR (ATR) 3304, 2930, 1649 cm^{-1}; MS (FAB) 286 (MH^+, 100); HRMS (ESI) calcd for $C_{17}H_{24}N_3O$ (MH^+) 286.1914, found 286.1908.

*1-(2-Iodophenyl)-3-phenylpropane-1,3-dione (**6**).* To a solution of LHMDS (15.2 mmol, 15.2 mL, 1.0 M solution in THF) in THF (20 mL) was added 2′-iodoacetophenone (**5**) (6.09 mmol, 1.50 g) at −78 °C, and the resulting mixture was stirred at −78 °C for 15 min. Benzoyl chloride (6.71 mmol. 780 μL) was then added to the mixture, and the resulting solution was stirred at room temperature for 2 h. The mixture was then quenched with saturated aqueous NH_4Cl solution, and the aqueous layer was extracted three times with AcOEt. The combined organic layers were washed with brine, dried over Na_2SO_4, and concentrated in vacuo to give the crude product as a residue, which was purified by silica gel chromatography (*n*-hexane/AcOEt = 12:1) to afford **6** (1.53 g, 72%): pale yellow oil; ^1H NMR ($CDCl_3$) δ 7.95−7.98 (m, 3H), 7.52−7.57 (m, 5H), 7.12−7.16 (t, J = 7.7 Hz, 1H), 6.57 (s, 1H) ppm (enol OH proton could not be observed); ^{13}C NMR ($CDCl_3$) δ 190.7, 183.7, 142.2, 140.5, 134.6, 132.7, 132.6, 129.2, 128.7, 128.2, 127.2, 97.8, 93.0 ppm; IR (ATR) 3046, 1595 cm^{-1}; MS (FAB) 351 (MH^+, 100); HRMS (ESI) calcd for $C_{15}H_{12}IO_2$ (MH^+) 350.9877, found 350.9872.

*Methyl 8-Iodo-1-oxo-1,2,3,4-tetrahydronaphthalene-2-carboxylate (**8**).* To a solution of NaH (19.2 mmol, 460 mg, 60% dispersion in mineral oil) in dimethyl carbonate (20 mL) was added a solution of **7**[31] (4.3 mmol, 500 mg) in dimethyl carbonate (10 mL) at room temperature. After being stirred at 70 °C for 2 h, the mixture was quenched with saturated aqueous NH_4Cl solution. The aqueous layer was extracted three times with AcOEt. The combined organic layers were washed with brine, dried over Na_2SO_4, and concentrated in vacuo. The residue was purified by silica gel chromatography (NH, *n*-hexane/AcOEt = 20:1) to afford **8** (1.21 g, 72%): pale yellow amorphous; ^1H NMR ($CDCl_3$)* major isomer δ 7.98 (d, J = 7.8 Hz, 1H), 7.24 (d, J = 7.8 Hz, 1H), 7.06 (dd, J = 7.8, 7.8 Hz, 1H), 3.78 (s, 3H) 3.68 (dd, J = 10.0, 4.9 Hz, 1H), 2.97−3.15 (m, 2H), 2.30−2.50 (m, 2H) ppm; minor isomer δ 7.92 (d, J = 7.8 Hz, 1H), 7.17 (d, J = 7.8 Hz, 1H), 6.91 (dd, J = 7.8, 7.8 Hz, 1H), 3.84 (s, 3H), 2.70 −2.74 (m, 2H), 2.42−2.51 (m, 2H) ppm (one peak of enol OH proton could not be observed); ^{13}C NMR (126 MHz, $CDCl_3$) δ 191.9, 173.1, 170.3, 164.7, 145.7, 143.2, 141.7, 141.5, 133.5, 131.9, 131.8, 130.9, 129.2, 127.6, 93.5, 90.5, 54.5, 52.5, 51.9, 29.4, 28.7, 25.5, 20.2 ppm (one peak of minor isomer could not be observed due to overlapping); IR (ATR) 2949, 1739, 1687 cm^{-1}; MS (FAB) 331 (MH^+, 100); HRMS (FAB) calcd for $C_{12}H_{12}IO_3$ (MH^+) 330.9831, found 330.9825. *Mixture of keto form (major) and enol form (minor).

*1-[3,5-Bis(trifluoromethyl)phenyl]-3-[2-[[2-(3-oxo-3-phenylpropanoyl)phenyl]ethynyl]phenyl]urea (**9**).* To a solution of **3** (0.54 mmol, 201 mg) and **6** (0.59 mmol, 207 mg) in THF/*i*-Pr_2NH (10 mL, 1: 1) were added $Pd(PPh_3)_2Cl_2$ (5 mol %, 19 mg) and CuI (10 mol %, 10 mg) successively at room temperature. After being stirred at room temperature for 1 h, the mixture was quenched with

dx.doi.org/10.1021/jo4028775 | J. Org. Chem. 2014, 79, 1805−1817

saturated aqueous NH_4Cl solution. The aqueous layer was extracted three times with AcOEt, and the combined organic layers were washed with brine, dried over Na_2SO_4, and concentrated in vacuo. The residue was purified by silica gel chromatography (*n*-hexane/AcOEt = 10: 1 → 5:1) to afford **9** (266 mg, 83%): yellow needles; mp 164−165 °C; ^{1}H NMR (pyridine-d_5) δ 8.86 (br, 1H), 8.75 (d, J = 8.3 Hz, 1H), 8.35 (s, 2H), 8.02 (d, J = 8.0 Hz, 2H), 7.99 (br, 1H), 7.70 (s, 1H), 7.63 (d, J = 7.7 Hz, 1H) 7.33−7.55 (m, 8H), 7.04 (dd, J = 7.7 Hz, 1H) ppm (two peaks could not be observed); ^{13}C NMR (pyridine-d_5) δ 186.7, 184.0, 152.3, 141.8, 140.7, 137.2, 133.8, 132.6, 131.9, 131.5, 131.3, 131.0, 130.8, 129.9, 128.9, 128.5, 128.4, 127.0. 126.6, 124.5, 123.2, 123.1, 122.4, 122.3, 122.1, 120.1, 119.0, 118.4, 114.8, 111.2, 96.5, 94.9, 90.2 ppm; IR (ATR) 3332, 2208, 1688, 1661, 1597 cm^{-1}; MS (FAB) 595 (MH^+, 45) 105 (100); HRMS (ESI) calcd for $C_{32}H_{21}F_6N_2O_3$ (MH^+) 595.1451, found 595.1453.

*Methyl 8-[[2-[3-[3,5-Bis(trifluoromethyl)phenyl]ureido]phenyl]-ethynyl]-1-oxo-1,2,3,4-tetrahydronaphthalene-2-carboxylate (**10**).* A procedure similar to that described for the preparation of **9** afforded **10** (152 mg, 60%): yellow prisms; mp 178−179 °C; ^{1}H NMR (500 MHz, $CDCl_3$) δ 9.24 (s, 1H), 8.73 (s, 1H), 8.50 (d, J = 8.3 Hz, 1H), 8.16 (s, 2H), 7.48−7.61 (m, 4H), 7.37 (dd, J = 7.9 Hz, 1H), 7.29 (d, J = 8.5 Hz, 1H), 7.01 (dd, J = 8.5 Hz, 1H), 3.78 (1H, dd, J = 9.2, 5.2 Hz), 3.64 (3H, s), 3.22−3.20 (1H, m), 3.10−3.04 (1H, m), 2.59−2.56 (1H, m), 2.48−2.43 (1H, m) ppm; ^{13}C NMR δ 194.9, 169.6, 152.4, 145.9, 142.1, 140.8, 133.9, 133.4, 132.3, 132.0, 131.8, 131.7, 131.5, 130.7, 130.5, 128.9, 124.4, 123.7, 122.3, 122.0, 119.2, 118.1,117.5,115.7, 110.7, 96.4, 91.6, 55.1, 52.6, 28.2, 25.8 (one peak could not be observed) ppm; IR (ATR) 3354, 2361, 1743, 1659, 1574 cm^{-1}; MS (FAB) 575 (MH^+, 100); HRMS (FAB) calcd for $C_{29}H_{21}F_6N_2O_4$ (MH^+) 575.1406, found 575.1402.

*1-[(1R,2R)-2-(Dimethylamino)cyclohexyl]-3-[2-[[2-(3-oxo-3-phenylpropanoyl)phenyl]ethynyl]phenyl]urea (**15**).* A procedure similar to that described for the preparation of **9** afforded **11** (132 mg, 75%): pale yellow prisms; mp 170−171 °C; $[\alpha]^{25}_D$ −23.5 (*c* 0,08, $CHCl_3$); ^{1}H NMR ($CDCl_3$) δ 8.20 (s, 1H), 8.13 (br, 1H), 8.02 (d, J = 8.3 Hz, 1H), 7.88 (d, J = 6.9 Hz, 2H), 7.60 (d, J = 7.8 Hz, 2H), 7.45−7.31 (m, 6H), 7.28−7.24 (m, 1H) 6.88 (dd, J = 7.5, 7.5 Hz, 1H), 6.31 (br, 1H), 5.01 (br, 1H), 3.78−3.75 (m, 1H), 3.49−3.46 (m, 1H), 2.52 (s, 6H), 2.52−2.46 (m, 1H), 2.05−1.80 (m, 3H), 1.56−1.30 (m, 4H) ppm (one peak of ammonium proton could not be observed); ^{13}C NMR ($CDCl_3$) δ 188.5, 184.1, 155.8, 145.4, 142.3, 140.4, 132.6, 132.4, 131.0, 130.6, 129.4, 128.7, 128.1, 127.8, 127.2, 127.0, 120.9, 118.6, 111.2, 96.8, 95.0, 89.2, 65.6, 51.1, 38.9, 33.6, 24.9, 24.5, 22.5 ppm; IR (ATR) 3265, 2144, 1783, 1686, 1601 cm^{-1}; MS (FAB) 508 (MH^+, 45), 136 (100); HRMS (FAB) calcd for $C_{32}H_{34}N_3O_3$ (MH^+) 508.2595, found 508.2598.

*Methyl 8-[[2-[3-[(1R,2R)-2-(Dimethylamino)cyclohexyl]ureido]-phenyl]ethynyl]-1-oxo-1,2,3,4-tetrahydronaphthalene-2-carboxylate (**12**).* A procedure similar to that described for the preparation of **9** afforded **12** (76 mg, 85%): yellow solid; mp 70−71 °C; ^{1}H NMR ($CDCl_3$)* major isomer 8.95 (1H, br s), 8.53 (1H, dd, J = 9.0 Hz), 7.58−7.56 (1H, m), 7.50−7.48 (1H, m), 7.44−7.43 (1H, m), 7.33−7.31 (1H, m), 7.27−7.24 (1H, m), 6.90−6.89 (1H, m), 6.47 (1H, d, J = 6.6 Hz), 3.78−3.76 (2H, m), 3.77 (3H, s), 3.14−3.12 (1H, m), 3.04−3.00 (1H, m), 2.61−2.23 (4H, m), 2.30 (6H, s), 1.87−1.80 (2H, m), 1.79−1.77 (1H, m), 1.27−1.15 (4H, m) ppm; minor isomer ^{1}H NMR ($CDCl_3$) δ 8.87 (1H, br s), 8.51 (1H, d, J = 8.9 Hz), 7.58−7.56 (1H, m), 7.50−7.48 (1H, m), 7.44−7.43 (1H, m), 7.33−7.31 (1H, m), 7.27−7.24 (1H, m), 6.90−6.89 (1H, m), 6.31 (1H, d, J = 6.6 Hz), 3.78−3.76 (2H, m), 3.77 (3H, s), 3.14−3.12 (1H, m), 3.04−3.00 (1H, m), 2.61−2.23 (4H, m), 2.30 (6H, s), 1.87−1.80 (2H, m), 1.79−1.77 (1H, m), 1.27−1.15 (4H, m) ppm; ^{13}C NMR ($CDCl_3$) δ 193.7, 193.1, 170.0, 155.5, 145.4, 144.9, 143.6, 143.5, 133.4, 133.3, 133.1, 132.9, 131.6, 131.5, 130.9, 130.6, 130.5, 130.4, 128.6, 128.5, 124.1, 123.7, 120.4, 120.4, 117.6, 117.5, 109.7, 109.7, 96.0, 95.7, 92.2, 91.9, 66.2, 66.0, 54.9, 54.8, 52.7, 52.6, 51.0, 50 0.8, 46.1, 40.3, 40.3, 34.1, 34.0, 28.0, 27.9, 26.0, 25.9, 25.3, 25.2, 24.9, 23.1, 22.8 ppm; IR (ATR) 3336, 2932, 2361, 1741, 1667, cm^{-1}; MS (FAB) 488 (MH^+, 100); HRMS (FAB) calcd for $C_{29}H_{34}N_3O_4$ (MH^+) 488.2549, found 488.2550. *Mixture of diastereomers.

Reaction of Binary-Complex Models 11 and 12. *General Procedure.* To a solution of **11** or **12** (1.0 equiv) in CD_2Cl_2 appropriate electrophile was added (1.5 equiv) at room temperature. After being stirred at room temperature for 10 or 30 min, the mixture was purified by silica gel chromatography ($CHCl_3$/MeOH). A general procedure afforded **14** (67%, 100% conversion)*: yellow amorphous solid; ^{1}H NMR ($CDCl_3$) δ: 8.49 (0.6H, d, J = 8.3 Hz), 8.44 (0.4H, d, J = 8.6 Hz), 8.04−7.98 (1H, br m), 7.92−7.84 (3H, m), 7.72−7.47 (3H, m), 7.40−6.83 (11H, m), 6.45−5.92 (2H, m), 5.54−5.58 (0.6H, br m), 5.51−5.53 (0.4H, br m), 3.78−3.74 (1H, m), 2.77−2.52 (1H, m), 2.25−1.70 (5H, m), 2.35 (3.6H, s), 2.20 (2.4H, s), 1.50−1.10 (4H, m), 1.25 (3.6H, s), 1.22 (5.4 H, s) ppm; HRMS (FAB) calcd for $C_{44}H_{49}N_4O_5$ (MH^+) 713.3703, found 713.3712. *Mixture of diastreomers (60:40).

*Methyl 2-[[(tert-Butoxycarbonyl)amino](phenyl)methyl)-8-[[2-[3-[(1R,2R)-2-(dimethylamino)cyclohexyl]ureido]phenyl]ethynyl]-1-oxo-1,2,3,4-tetrahydronaphthalene-2-carboxylate (**15**).* A general procedure afforded 15 (77%, 100% conversion): yellow amorphous; $[\alpha]^{25}_D$ +88.4 (*c* 1.12, $CHCl_3$); ^{1}H NMR ($CDCl_3$) δ 8.54 (1H, d, J = 8.6 Hz), 8.49 (1H, s), 7.55 (1H, d, J = 7.7 Hz), 7.48 (1H, d, J = 7.7 Hz), 7.46−7.44 (1H, m), 7.38 (2H, d, J = 7.4 Hz), 7.32−7.24 (5H, m), 6.92 (1H, td, J = 7.5, 1.1 Hz), 6.54 (1H, br s), 6.07 (1H, br s), 5.54 (1H, br s), 3.86−3.84 (1H, br m), 3.72 (3H, s), 3.25−3.00 (3H, m), 2.76−2.70 (1H, m), 2.32 (6H, s), 2.26−2.24 (2H, m), 2.00−1.65 (3H, m), 1.40−1.25 (4H, m), 1.25 (9H, s) ppm; ^{13}C NMR ($CDCl_3$) δ 194.2, 170.6, 155.5, 155.2, 143.4, 143.0, 137.8, 133.0, 131.9, 130.3, 130.2, 128.9, 128.5 (×2), 128.3, 127.9, 123.8, 120.7, 118.2, 110.2, 95.7, 91.5, 79.9, 65.0, 63.0, 55.6, 52.8, 51.5, 40.3, 34.1, 28.1, 27.9, 27.2, 25.8, 25.3 (×2) ppm; IR (ATR) 3393, 3339, 2200, 1733, 1664, 1525 cm^{-1}; MS (FAB) 693 (MH^+, 87), 57 (100); HRMS (FAB) calcd for $C_{41}H_{49}N_4O_6$ (MH^+) 693.3652, found 693.3647.

*Di-tert-butyl 1-[(S)-8-[[2-[3-[(1R,2R)-2-(Dimethylamino)-cyclohexyl]ureido]phenyl]ethynyl]-2-(methoxycarbonyl)-1-oxo-1,2,3,4-tetrahydronaphthalen-2-yl]hydrazine-1,2-dicarboxylate) (**17**).* A general procedure afforded 17 (96%, 100% conversion): yellow amorphous; $[\alpha]^{25}_D$ +9.4 (*c* 0.80, $CHCl_3$); ^{1}H NMR ($CDCl_3$, 60 °C) δ 8.63 (1H, s), 8.48 (1H, d, J = 8.0 Hz), 7.48−7.39 (3H, m), 7.32−7.23 (2H, m), 6.89 (1H, t, J = 7.4 Hz), 5.59 (1H, br s), 3.85 (3H, s), 3.84−3.82 (1H, m), 3.68−3.60 (1H, m), 3.36−3.20 (1H, br m), 3.04−2.98 (1H, m), 2.95−2.91 (1H, m), 2.72−2.66 (1H, m), 2.27−2.23 (1H, m), 2.26 (6H, s), 1.97−1.92 (1H, m), 1.84−1.80 (1H, m), 1.73−1.68 (1H, m), 1.44 (9H, s), 1.42−1.15 (4H, m), 1.14 (9H, s) ppm (one peak of NH proton could not be observed); ^{13}C NMR ($CDCl_3$, 60 °C) δ 190.7, 170.3, 155.3, 154.8, 147.2, 142.9, 133.0, 132.4, 131.4, 130.2, 130.1, 128.5, 124.2, 120.7, 118.6, 110.6, 95.6, 91.8, 82.6, 80.6, 76.6, 64.0, 52.9, 52.2, 39.9, 34.3, 30.3, 28.1, 27.9, 26.2, 25.6, 25.5, 21.8 ppm (one peak could not be observed); IR (ATR) 3407, 3346, 2933, 1747. 1717, 1671, 1524 cm^{-1}; MS (FAB) 718 (MH^+, 100); HRMS (ESI) calcd for $C_{39}H_{52}N_5O_8$ (MH^+) 718.3810, found 718.3809.

*(S)-Di-tert-butyl 1-[8-Iodo-2-(methoxycarbonyl)-1-oxo-1,2,3,4-tetrahydronaphthalen-2-yl]hydrazine-1,2-dicarboxylate (**19**).*[20] To a solution of **8** (1.0 equiv) and catalyst (0.1 equiv) in CH_2Cl_2 was added **16** (2.0 equiv) at an appropriate temperature. After being stirred at room temperature for 12 h, the mixture was concentrated in vacuo. The residue was purified by silica gel chromatography (*n*-hexane/AcOEt = 7:1): white solid; mp 61−62 °C; $[\alpha]^{25}_D$ +10.6 (53% ee, *c* 0.74, $CHCl_3$); ^{1}H NMR ($CDCl_3$, 60 °C) δ 7.86−7.81 (1H, br m), 7.23 (1H, d, J = 7.4 Hz), 7.01 (1H, t, J = 7.4 Hz), 6.46 (1H, br s), 3.85 (3H, s), 3.50−3.40 (1H, br m), 3.12−3.05 (1H, br m), 2.98−2.93 (1H, m), 2.66−2.60 (1H, m), 1.44 (9H, s), 1.25 (9H, s) ppm; ^{13}C NMR ($CDCl_3$, 60 °C) δ 189.7, 170.1, 155.6, 146.1, 140.5, 132.8, 128.8, 93.9, 87.6, 83.0, 81.1, 76,2, 52.7, 30.7, 28.2, 28.0, 27.9, 26.3 ppm; IR (ATR) 3309, 2979, 1721 cm^{-1}; MS (FAB) 561 (MH^+, 11), 449 (100); HRMS (FAB) calcd for $C_{22}H_{30}IN_2O_7$ (MH^+) 561.1098, found 561.1102; HPLC [Chiralpak AD, *n*-hexane/2-propanol = 95/5, 1.0 mL/min, λ = 254 nm, retention times: (major) 15.8 min (minor) 35.2 min].

*(S)-Methyl 2-[(R)-[(tert-Butoxycarbonyl)amino](phenyl)methyl]-8-iodo-1-oxo-1,2,3,4-tetrahydronaphthalene-2-carboxylate (**22**).*[22] To a solution of **8** (1.0 equiv) and catalyst (0.1 equiv) in CH_2Cl_2 was added **13** (1.2 equiv) at an appropriate temperature. After being stirred at room temperature for 12 h, the mixture was concentrated in

dx.doi.org/10.1021/jo4028775 | J. Org. Chem. 2014, 79, 1805−1817

vacuo. The residue was purified by silica gel chromatography (*n*-hexane/AcOEt = 5:1): white solid; mp 161−162 °C; $[\alpha]^{25}_{D}$ −0.17 (77% ee, *c* 2.50, $CHCl_3$); ^{1}H NMR ($CDCl_3$) δ 7.91 (1H, d, *J* = 7.7 Hz), 7.43 (2H, d, *J* = 6.9 Hz), 7.31 (2H, dd, *J* = 7.4, 7.4 Hz), 7.26 (1H, t, *J* = 7.4 Hz), 7.20 (1H, d, *J* = 7.4 Hz), 7.05 (1H, t, *J* = 7.7 Hz), 6.33 (1H, br s), 5.21 (1H, d, *J* = 10.3 Hz), 3.53 (3H, s), 3.16−3.13 (2H, m), 2.67−2.65 (1H, m), 2.30−2.28 (1H, m), 1.36 (9H, s) ppm; ^{13}C NMR ($CDCl_3$) δ 195.3, 170.5, 155.0, 143.5, 140.9, 138.4, 133.7, 133.1, 129.0, 128.3, 128.3, 127.8, 99.9, 79.7, 63.0, 57.2, 52.4, 29.2, 28.3, 26.2 ppm; IR (ATR) 3436, 2978, 1698 cm^{-1}; MS (FAB) 536 (MH^+,7), 206 (100); HRMS (FAB) calcd for $C_{24}H_{27}INO_5$ (MH^+) 536.0934, found 536.0933; HPLC HPLC [Chiralpak AD, *n*-hexane/2-propanol = 95/5, 1.0 mL/min, λ = 254 nm, retention times: (major) 18.0 min (minor) 45.0 min].

Determination of the Absolute Configuration of 15 and 17. A procedure similar to that described for the preparation of **9** afforded the mixture of **17** and **20**. When **19** (er = 76.5:23.5) was used as a substrate, the ratio **17**/**20** in the resulting mixture was 76:24. When racemic **19** was used as a substrate, the ratio **17**/**20** in the resulting mixture was 50:50.

*Mixture of **17** and **20** (50:50):* ^{1}H NMR ($CDCl_3$, 60 °C) δ 8.65 (0.5H, br s), 8.49 (0.5H, d, *J* = 8.0 Hz), 8.38 (0.5H, d, *J* = 8.0 Hz), 8.26 (0.5H, br s), 7.48−7.23 (5.0H, m), 6.89 (1H, t, *J* = 7.4 Hz), 6.69 (0.5H, br s), 5.81(0.5H, br s), 5.59 (0.5H, br s), 3.87 (1.5H, s), 3.85 (1.5H, s), 3.84−3.82 (1H, m), 3.68−3.20 (2H, br m), 3.04−2.23 (4H, m), 2.26 (3H, s), 2.24 (3H, s), 1.97−1.68 (3H, m), 1.44 (9H, s), 1.42−1.15 (4H, m), 1.14 (9H, s) ppm (one peak of NH proton of **17** could not be observed).

*(1R,2S)-Methyl 2-[(R)-[(tert-Butoxycarbonyl)amino](phenyl)-methyl]-8-[[2-[3-[(1R,2R)-2-(dimethylamino)cyclohexyl]ureido]-phenyl]ethynyl]-1-hydroxy-1,2,3,4-tetrahydronaphthalene-2-carboxylate (**21**).* To a solution of **15** (0.1 mmol) in MeOH (2.0 mL) was added $NaBH_4$ (1.0 mmol) at room temperature. After being stirred at room temperature for 1 h, the mixture was quenched with saturated aqueous NH_4Cl solution. The aqueous layer was extracted three times with AcOEt, and the combined organic layers were washed with brine, dried over Na_2SO_4, and concentrated in vacuo. The residue was purified by silica gel chromatography ($CHCl_3$/MeOH/NEt_3= 50:1:0.1 → 20:1:0.1) to afford 21 (77%): white solid; mp 152−154 °C; $[\alpha]^{25}_{D}$ −85.6 (*c* 0.67, $CHCl_3$); ^{1}H NMR ($CDCl_3$) δ: 7.90 (1H, d, *J* = 8.3 Hz), 7.53 (1H, br s), 7.35−7.11 (9H, m), 7.01 (1H, d, *J* = 7.5 Hz), 6.93 (1H, d, *J* = 7.5 Hz), 6.31 (1H, d, *J* = 9.7 Hz), 5.92−5.90 (1H, br m), 5.41−5.39 (2H, br m), 5.15 (1H, d, *J* = 9.7 Hz), 3.52−3.47 (1H, br m), 3.41 (3H, s), 2.80−2.78 (2H, m), 2.38−1.95 (4H, m), 1.87 (6H, s), 1.78−1.59 (3H, m), 1.26 (9H, s), 1.25−1.00 (4H, m) ppm; ^{13}C NMR ($CDCl_3$) δ: 173.1, 155.9, 155.7, 141.7, 138.5, 137.7, 136.1, 130.8, 129.9, 129.4, 129.3, 128.2, 128.0, 127.8, 127.5, 123.8, 122.0, 121.0, 112.8, 92.7, 90.4, 79.8, 67.4, 66.3, 59.5, 54.7, 51.8, 51.7, 39.3, 34.3, 28.3, 26.3, 25.1, 24.8, 22.9, 21.1 ppm; IR (ATR) 3358, 2934, 1716 cm^{-1}; MS (FAB) 695 (MH^+, 100); HRMS (ESI) calcd for $C_{41}H_{51}N_4O_6$ (MH^+) 695.3803, found 695.3812.

*(1S,2S)-Methyl 2-[(R)-[(tert-Butoxycarbonyl)amino](phenyl)-methyl]-1-hydroxy-8-iodo-1,2,3,4-tetrahydronaphthalene-2-carboxylate (**23**).* To a solution of **22** (0.2 mmol, 107 mg) in MeOH (2.0 mL) was added $NaBH_4$ (1.0 mmol, 38 mg) at room temperature. After being stirred at room temperature for 1 h, the mixture was quenched with saturated aqueous NH_4Cl solution. The aqueous layer was extracted three times with AcOEt, and the combined organic layers were washed with brine, dried over Na_2SO_4, and concentrated in vacuo. The residue was purified by silica gel chromatography (*n*-hexane/AcOEt = 3:1) to afford **23** (82 mg, 76%). The residue after evaporation included **23** and **25** (80:20). Only **23** could be isolated in 76% yield as a pure form: white solid; mp 176−177 °C; $[\alpha]^{25}_{D}$ −86.6 (*c* 1.42, 91% ee, $CHCl_3$); ^{1}H NMR ($CDCl_3$) δ 7.67 (1H, d, *J* = 7.7 Hz), 7.36−7.31 (3H, m), 7.16 (2H, d, *J* = 6.9 Hz), 7.03 (1H, d, *J* = 7.7 Hz), 6.86 (1H, t, *J* = 7.7 Hz), 5.93 (1H, d, *J* = 10.3 Hz), 5.22 (1H, s), 5.09 (1H, d, *J* = 10.3 Hz), 4.34 (1H, br s), 3.46 (3H, s), 2.85−2.82 (2H, m), 2.24−2.20 (1H, m), 1.82−1.77 (1H, m), 1.51 (9H, s) ppm; ^{13}C NMR ($CDCl_3$) δ 172.7, 156.7, 138.5, 138.1, 137.8, 137.2, 129.6, 129.3, 128.3, 128.0, 127.5, 103.2, 80.7, 73.1, 58.7, 55.7, 51.6, 28.5, 26.8, 22.7 ppm; IR (ATR) 3422, 1712, 1687 cm^{-1}; MS (FAB) 538 (MH^+,4), 106 (100); HRMS (FAB) calcd for $C_{24}H_{29}INO_5$ (MH^+) 538.1090, found 538.1092.

*(1S,2R)-Methyl 2-[(S)-[(tert-Butoxycarbonyl)amino](phenyl)-methyl]-8-[[2-[3-[(1R,2R)-2-(dimethylamino)cyclohexyl]ureido]-phenyl]ethynyl]-1-hydroxy-1,2,3,4-tetrahydronaphthalene-2-carboxylate (**24**).* A procedure similar to that described for the preparation of **9** afforded the mixture of **21** and **24**. When **23** (er = 95.5:4.5) was used as substrate, only **21** was isolated in 84% yield. When racemic **23** was used as a substrate, **21** and **24** were isolated in 46% and 42% yields, respectively: white solid; mp 154−156 °C; $[\alpha]^{25}_{D}$ +130.4 (*c* 0.32, $CHCl_3$); ^{1}H NMR ($CDCl_3$) δ 8.35 (1H, d, *J* = 8.6 Hz), 7.45 (1H, d, *J* = 7.4 Hz), 7.38 (1H, d, *J* = 7.4 Hz), 7.32−7.16 (8H, m), 7.08 (1H, d, *J* = 8.0 Hz), 6.97 (1H, t, *J* = 7.4 Hz), 6.23−6.07 (2H, br m), 5.60 (1H, s), 5.14 (1H, d, *J* = 9.2 Hz), 3.44 (3H, s), 3.41−3.36 (1H, m), 2.99−2.96 (1H, m), 2.85−2.78 (1H, m), 2.68−2.09 (10H, m), 2.02−1.64 (3H, m), 1.40−1.08 (4H, m), 1.25 (9H, s) ppm (one peak of OH proton could not be observed); ^{13}C NMR ($CDCl_3$) δ 173.6, 156.6, 155.5, 141.4, 137.3, 136.6, 131.5, 129.6, 128.3, 128.2, 127.9, 127.5, 121.3, 118.3, 110.9, 89.3, 80.4, 67.9, 66.0, 51.7, 31.9, 31.6, 29.7, 28.1, 25.9, 24.7, 22.7, 22.3, 21.0, 14.1 ppm (six peaks could not be observed due to overlapping); IR (ATR) 3348, 2951, 1704 cm^{-1}; MS (FAB) 695 (MH^+, 100); HRMS (ESI) calcd for $C_{41}H_{51}N_4O_6$ (MH^+) 695.3804, found 695.3810.

■ ASSOCIATED CONTENT

Ⓢ Supporting Information

Results of catalyst screening in hydrazination and Mannich reaction of **8**, copies of ^{1}H and ^{13}C NMR spectra for all new compounds, and the computational details, and X-ray crystal structures analysis data of **9K**, **10**, and **11E** (CIF). This material is available free of charge via the Internet at http://pubs.acs.org.

■ AUTHOR INFORMATION

Corresponding Author

*E-mail: takemoto@pharm.kyoto-u.ac.jp.

Notes

The authors declare no competing financial interest.

■ ACKNOWLEDGMENTS

We gratefully acknowledge a Grant-in-Aid for Scientific Research (Y.T.) on Innovative Areas "Advanced Molecular Transformations by Organocatalysts" from MEXT (Japan) and the Japan Society for the Promotion of Science (JSPS) Research Fellowship for Young Scientists (T.A.).

■ REFERENCES

(1) (a) Jencks, W. P. *Catalysis in Chemistry and Enzymology*; McGraw-Hill: New York, 1969. (b) Hedstrom, L. *Chem. Rev.* **2002**, *102*, 4501−4524. (c) Ekici, O. D.; Paetzel, M.; Dalbey, R. E. *Protein Sci.* **2008**, *17*, 2023−2037. (d) Knowles, R. R.; Jacobsen, E. N. *Proc. Natl. Acad. Sci. U.S.A.* **2010**, *107*, 20678−20685. (e) Berg, J. M.; Tymoczko, J. L.; Stryer, L. *Biochemistry*, 7th ed.; W. H. Freeman and Co.: New York, 2012.

(2) For recent books, see: (a) Berkessel, A.; Gröger, H. *Asymmetric Organocatalysis*; Wiley−VCH: Weinheim, 2005. (b) Shibasaki, M. *New Development of Organocatalyst*; CMC Publisher: Tokyo, 2006. (c) *Enantioselective Organocatalysis*; Dalko, P. I., Ed.; Wiley-VCH: Weinheim, 2007. (d) *Organocatalysis*; Reetz, M. T., List, B., Jaroch, S., Weinmann, H., Eds.; Springer: Berlin, 2008. (e) List, B.; Maruoka, K. *Science of Synthesis Asymmetric Organocatalysis*; Thieme: Stuttgart, 2012. For selected recent reviews on organocatalysts, see: (f) List, B., Eds. *Chem. Rev.* **2007**, *107*, 5413−5883. (g) Barbas, C. F., III *Angew. Chem., Int. Ed.* **2008**, *47*, 42−47. (h) Dondoni, A.; Massi, A. *Angew. Chem., Int. Ed.* **2008**, *47*, 4638−4660. (i) MacMillan, D. W. C. *Nature* **2008**, *455*, 304−308. (j) Melchiorre, P.; Marigo, M.; Carlone, A.; Bartoli, G. *Angew. Chem., Int. Ed.* **2008**, *47*, 6138−6171. (k) Grondal,

C.; Jeanty, M.; Enders, D. *Nat. Chem.* **2010**, *2*, 167−178. (l) Palomo, C.; Oiarbide, M.; López, R. *Chem. Soc. Rev.* **2009**, *38*, 632−653. (m) Giacalone, F.; Gruttadauria, M.; Agrigento, P.; Noto, R. *Chem. Soc. Rev.* **2012**, *41*, 2406−2447. (n) Pellissier, H. *Adv. Synth. Catal.* **2012**, *354*, 237−294. (o) Wende, R .C.; Schreiner, P. R. *Green Chem.* **2012**, *14*, 1821−1849. (p) Li, J.-L.; Liu, T.-Y.; Chen, Y.-C. *Acc. Chem. Res.* **2012**, *45*, 1491−1500. (q) Marson, C. M. *Chem. Soc. Rev.* **2012**, *41*, 7712−7722.

(3) For a review, see: (a) Cheong, P. H.-Y.; Legault, C. Y.; Um, J. M.; Çelebi-Ölçüm, N.; Houk, K. N. *Chem. Rev.* **2011**, *111*, 5042−5137. For selected recent examples, see: (b) Nielsen, M.; Worgull, D.; Zweifel, T.; Gschwend, B.; Bertelsen, S.; Jørgensen, K. A. *Chem. Commun.* **2011**, *47*, 632−649. (c) Moran, A.; Hamilton, A.; Bo, C.; Melchiorre, P. *J. Am. Chem. Soc.* **2013**, *135*, 9091−9098. (d) Yang, C.; Xue, X.-S.; Jin, J.-L.; Li, X.; Cheng, J.-P. *J. Org. Chem.* **2013**, *78*, 7076−7085.

(4) For pioneering work on thiourea catalysts, see: (a) Sigman, M. S.; Jacobsen, E. N. *J. Am. Chem. Soc.* **1998**, *120*, 4901−4902. (b) Sigman, M. S.; Vachal, P.; Jacobsen, E. N. *Angew. Chem., Int. Ed.* **2000**, *39*, 1279−1281. (c) Schreiner, P. R.; Wittkopp, A. *Org. Lett.* **2002**, *4*, 217−220. (d) Wittkopp, A.; Schreiner, P. R. *Chem. −Eur. J.* **2003**, *9*, 407−414. For reviews of bifunctional amino(thio)urea catalysts, see: (e) Connon, S. J. *Chem.—Eur. J.* **2006**, *12*, 5418−5427. (f) Doyle, A. G.; Jacobsen, E. N. *Chem. Rev.* **2007**, *107*, 5713−5743. (g) Connon, S. J. *Chem. Commun.* **2008**, 2499−2510. (h) Zhang, Z.; Schreiner, P. R. *Chem. Soc. Rev.* **2009**, *38*, 1187−1198. (i) Takemoto, Y. *Chem. Pharm. Bull.* **2010**, *58*, 593−601.

(5) For our selected previous works, see: (a) Okino, T.; Hoashi, Y.; Takemoto, Y. *J. Am. Chem. Soc.* **2003**, *125*, 12672−12673. (b) Okino, T.; Nakamura, S.; Furukawa, T.; Takemoto, Y. *Org. Lett.* **2004**, *6*, 625−627. (c) Hoashi, Y.; Okino, T.; Takemoto, Y. *Angew. Chem., Int. Ed.* **2005**, *44*, 4032−4035. (d) Okino, T.; Hoashi, Y.; Furukawa, T.; Xuenong, X.; Takemoto, Y. *J. Am. Chem. Soc.* **2005**, *127*, 119−125. (e) Xu, X.; Yabuta, T.; Yuan, P.; Takemoto, Y. *Synlett* **2006**, 137−140. (f) Inokuma, T.; Hoashi, Y.; Takemoto, Y. *J. Am. Chem. Soc.* **2006**, *128*, 9413−9419. (g) Yamaoka, Y.; Miyabe, H.; Takemoto, Y. *J. Am. Chem. Soc.* **2007**, *129*, 6686−6687. (h) Yamaoka, Y.; Miyabe, H.; Yasui, Y.; Takemoto, Y. *Synthesis* **2007**, 2571−2575. (i) Inokuma, T.; Takasu, K.; Sakaeda, T.; Takemoto, Y. *Org. Lett.* **2009**, *11*, 2425−2428.

(6) For selected examples of bifunctional (thio)urea organocatalysts, see: (a) Sohtome, Y.; Hashimoto, Y.; Nagasawa, K. *Adv. Synth. Catal.* **2005**, *347*, 1643−1648. (b) Herrera, R. P.; Sgarzani, V.; Bernardi, L.; Ricci, A. *Angew. Chem., Int. Ed.* **2005**, *44*, 6576−6579. (c) Wang, J.; Li, H.; Yu, X.; Zu, Li.; Wang, W. *Org. Lett.* **2005**, *7*, 4293−4296. (d) Vakulya, B.; Varga, S.; Csámpai, A.; Soós, T. *Org. Lett.* **2005**, *7*, 1967−1969. (e) Cao, C.-L.; Ye, M.-C.; Sun, X.-L.; Tang, Y. *Org. Lett.* **2006**, *8*, 2901−2904. (f) Berkessel, A.; Roland, K.; Neudörfl, J. M. *Org. Lett.* **2006**, *8*, 4195. (g) Marcelli, T.; van der Haas, R. N. S.; van Maarseveen, J. H.; Hiemstra, H. *Angew. Chem., Int. Ed.* **2006**, *45*, 929−931. (h) Liu, K.; Cui, H.-F.; Nie, J.; Dong, K.-Y.; Li, X.-J.; Ma, J.-A. *Org. Lett.* **2007**, *9*, 923−925. (i) Robak, M. T.; Trincado, M.; Ellman, J. A. *J. Am. Chem. Soc.* **2007**, *129*, 15110−15111. (j) Li, L.; Klauber, E. G.; Seidel, D. *J. Am. Chem. Soc.* **2008**, *130*, 12248−12249. (k) So, S. S.; Burkett, J. A.; Mattson, A. E. *Org. Lett.* **2011**, *13*, 716−719. (l) Probst, N.; Madarász, Á.; Valkonen, A.; Pápai, I.; Rissanen, K.; Neuvonen, A.; Pihko, P. M. *Angew. Chem., Int. Ed.* **2012**, *51*, 8495−8499. (m) Jörres, M.; Schiffers, I.; Atodiresei, I.; Bolm, C. *Org. Lett.* **2012**, *14*, 4518−4521. (n) Núñez, M. G.; Farley, A. J. M.; Dixon, D. J. *J. Am. Chem. Soc.* **2013**, *135*, 16348−16351.

(7) For recent examples of bifunctional HB-donor organocatalysts bearing different scaffolds, see: (a) Malerich, J. P.; Hagihara, K.; Rawal, V. H. *J. Am. Chem. Soc.* **2008**, *130*, 14416−14417. (b) Almaşi, D.; Alonso, D. A.; Gómez-Bengoa, E.; Nájera, C. *J. Org. Chem.* **2009**, *74*, 6163−6168. (c) Zhang, L.; Lee, M.-M.; Lee, S.-M.; Lee, J.; Cheng, M.; Jeong, B.-S.; Park, H.-g.; Jew, S.-s. *Adv. Synth. Catal.* **2009**, *351*, 3063. (d) Inokuma, T.; Furukawa, M.; Uno, T.; Suzuki, T.; Yoshida, K.; Yano, T.; Matsuzaki, K.; Takemoto, Y. *Chem.—Eur. J.* **2011**, *17*, 10470−10477. (e) Inokuma, T.; Furukawa, M.; Suzuki, Y.; Kimachi, T.; Kobayashi, Y.; Takemoto, Y. *ChemCatChem* **2012**, *4*, 983−985. (f) Kobayashi, Y.; Taniguchi, Y.; Hayama, N.; Inokuma, T.; Takemoto, Y. *Angew. Chem., Int. Ed.* **2013**, *52*, 11114−11118.

(8) For selected theoretical works on bifunctional thiourea organocatalysis, see: (a) Zhu, Y.; Drueckhammer, D. G. *J. Org. Chem.* **2005**, *70*, 7755−7760. (b) Yalalov, D. A.; Tsogoeva, S. B.; Schmatz, S. *Adv. Synth. Catal.* **2006**, *348*, 826−832. (c) Zhu, R.; Zhang, D.; Wu, J.; Liu, C. *Tetrahedron: Asymmetry* **2006**, *17*, 1611−1616. (d) Hamza, A.; Schubert, G.; Soós, T.; Pápai, I. *J. Am. Chem. Soc.* **2006**, *128*, 13151−13160. (e) Hammar, P.; Marcelli, T.; Hiemstra, H.; Himo, F. *Adv. Synth. Catal.* **2007**, *349*, 2537−2548. (f) Zuend, S. J.; Jacobsen, E. N. *J. Am. Chem. Soc.* **2007**, *129*, 15872−15883. (g) Chen, D.; Lu, N.; Zhang, G.; Mi, S. *Tetrahedron: Asymmetry* **2009**, *20*, 1365−1368. (h) Simón, L.; Goodman, J. M. *Org. Biomol. Chem.* **2009**, *7*, 483−487. (i) Xu, H.; Zuend, S. J.; Woll, M. G.; Tao, Y.; Jacobsen, E. N. *Science* **2010**, *327*, 986−990. (j) Tan, B.; Lu, Y. P.; Zeng, X.; Chua, P. J.; Zhong, G. *Org. Lett.* **2010**, *12*, 2682−2685. (k) Manzano, R.; Andrés, J. M.; Álvarez, R.; Muruzábal, M. D.; de Lera, Á. R.; Pedrosa, R. *Chem.−Eur. J.* **2011**, *17*, 5931−5938. (l) Li, X.; Xue, X.-S.; Liu, C.; Wang, B.; Tan, B.-X.; Jin, J.-L.; Zhang, Y.-Y.; Dong, N.; Cheng, J.-P. *Org. Biomol. Chem.* **2012**, *10*, 413−420. (m) Shubina, T. E.; Freund, M.; Schenker, S.; Clark, T.; Tsogoeva, S. B. *Beilstein J. Org. Chem.* **2012**, *8*, 1485−1498. (n) Zhu, J.-L.; Zhang, Y.; Liu, C.; Zheng, A.-M.; Wang, W. *J. Org. Chem.* **2012**, *77*, 9813−9825. (o) Sengupta, A.; Sunoj, R. B. *J. Org. Chem.* **2012**, *77*, 10525−10536.

(9) For reviews, see: (a) Notz, W.; Tanaka, F.; Barbas, C. F., III. *Acc. Chem. Res.* **2004**, *37*, 580−591. (b) Guillena, G.; Ramón, D. J. *Tetrahedron: Asymmetry* **2006**, *17*, 1465−1492. (c) Mukherjee, S.; Yang, J. W.; Hoffmann, S.; List, B. *Chem. Rev.* **2007**, *107*, 5471−5569. (d) Ouellet, S. G.; Walji, A. M.; MacMillan, D. W. C. *Acc. Chem. Res.* **2007**, *40*, 1327−1339. (e) Yang, H.; Carter, R. G. *Synlett* **2010**, 2827−2838. (f) Shoji, M.; Hayashi, Y. In *Modern Tools for the Synthesis of Complex Bioactive Molecules*; Cossy, J., Arseniyadis, S., Eds.; John Wiley & Sons: Hoboken, 2012; 189−212. (g) Xu, L.-W.; Li, L.; Shi, Z.-H. *Adv. Synth. Catal.* **2010**, *352*, 243−279. (h) Albrecht, Ł.; Jiang, H.; Jørgensen, K. A. *Angew. Chem., Int. Ed.* **2011**, *50*, 8492−8509. (i) Jensen, K. L.; Dickmeiss, G.; Jiang, H.; Albrecht, Ł.; Jørgensen, K. A. *Acc. Chem. Res.* **2012**, *45*, 248−264.

(10) Ammonium enolates have been described in several reports, see: (a) Reetz, M. T.; Hütte, S.; Goddard, R.; Robyr, R. *Chem.—Eur. J.* **1996**, *2*, 382−384. (b) Nishiwaki, N.; Nishida, D.; Ohnishi, T.; Hidaka, F.; Shimizu, S.; Tamura, M.; Hori, K.; Tohda, Y.; Ariga, M. *J. Org. Chem.* **2003**, *68*, 8650−8656.

(11) (a) Iwasawa, T.; Hooley, R. J.; Rebek, J., Jr. *Science* **2007**, *317*, 493−496. (b) Hooley, R. J.; Rebek, J., Jr. *Chem. Biol.* **2009**, *16*, 255−264. (c) Ohashi, Y. *Chem. Rec.* **2013**, *13*, 303−325.

(12) (a) Kemp, D. S.; Li, Z. Q. *Tetrahedron Lett.* **1995**, *36*, 4175−4178. (b) Kemp, D. S.; Li, Z. Q. *Tetrahedron Lett.* **1995**, *36*, 4179−4180.

(13) (a) Yang, X. W.; Yuan, L. H.; Yamamoto, K.; Brown, A. L.; Feng, W.; Furukawa, M.; Zeng, X. C.; Gong, B. *J. Am. Chem. Soc.* **2004**, *126*, 3148−3162. (b) Cary, J. M.; Moore, J. S. *Org. Lett.* **2002**, *4*, 4663−4666. (c) Yang, X. W.; Brown, A. L.; Furukawa, M.; Li, S. J.; Gardinier, W. E.; Bukowski, E. J.; Bright, F. V.; Zheng, C.; Zeng, X. C.; Gong, B. *Chem. Commun.* **2003**, 56−57. (d) Hu, W.; Zhu, N. B.; Tang, W.; Zhao, D. H. *Org. Lett.* **2008**, *10*, 2669−2672. (e) Wyrembak, P. N.; Hamilton, A. D. *J. Am. Chem. Soc.* **2009**, *131*, 4566−4567. (f) Jo, J.; Lee, D. *J. Am. Chem. Soc.* **2009**, *131*, 16283−16291. (g) Jones, I. M.; Hamilton, A. D. *Org. Lett.* **2010**, *12*, 3651−3653. (h) Jones, I. M.; Hamilton, A. D. *Angew. Chem., Int. Ed.* **2011**, *50*, 4597−4600. (i) Jones, I. M.; Lingard, H.; Hamilton, A. D. *Angew. Chem., Int. Ed.* **2011**, *50*, 12569−12571.

(14) Urea-type catalysts have been reported to function in a similar manner to thiourea-type catalysts, see: ref 4 and references cited therein.

(15) Sonogashira, K.; Tohda, Y.; Hagihara, N. *Tetrahedron Lett.* **1975**, *16*, 4467−4470.

(16) The ^{1}H NMR spectrum estimated in $CDCl_3/D_2O$ (15:1) revealed the disappearance of one proton peak located in the range of 7.80−8.00 ppm.

(17) For selected recent reports on alkyne distortion, see: (a) Shapiro, N. D.; Toste, F. D. *Proc. Nat. Acad. Sci. U.S.A.* **2008**, *105*, 2779−2782. (b) Fischer, F. R.; Nuckolls, C. *Angew. Chem., Int. Ed.* **2010**, *49*, 7257−7260. (c) Heiner, D. In *Targets in Heterocyclic Systems*; Royal Society of Chemistry: Italy, 2011; Vol. *15*, pp 1−49.
(18) The ammonium−enolate complex model lies 3.9 kcal/mol below the amine−enol complex model.
(19) We used aminobenzothiadiazine **18** as a catalyst instead of aminothiourea **1** because **1** gradually decomposed under the reaction conditions.
(20) Several trials were unsuccessful, probably because of the steric hindrance of the iodine group. The full details are described in the Supporting Information.
(21) When racemic **19** was used as a substrate, the ratio **17** to **20** in the resulting mixture was 50:50.
(22) The details of trials aimed at improving the enantioselectivity of the Mannich reaction are described in the Supporting Infomation.
(23) When racemic **23** was used as a substrate, **21** and **24** were obtained in 46 and 42% yields, respectively.
(24) Gaussian 09, Revision B.01: Frisch, M. J.; Trucks, G. W.; Schlegel, H. B.; Scuseria, G. E.; Robb, M. A.; Cheeseman, J. R.; Scalmani, G.; Barone, V.; Mennucci, B.; Petersson, G. A.; Nakatsuji, H.; Caricato, M.; Li, X.; Hratchian, H. P.; Izmaylov, A. F.; Bloino, J.; Zheng, G.; Sonnenberg, J. L.; Hada, M.; Ehara, M.; Toyota, K.; Fukuda, R.; Hasegawa, J.; Ishida, M.; Nakajima, T.; Honda, Y.; Kitao, O.; Nakai, H.; Vreven, T.; Montgomery, J. A., Jr.; Peralta, J. E.; Ogliaro, F.; Bearpark, M.; Heyd, J. J.; Brothers, E.; Kudin, K. N.; Staroverov, V. N.; Kobayashi, R.; Normand, J.; Raghavachari, K.; Rendell, A.; Burant, J. C.; Iyengar, S. S.; Tomasi, J.; Cossi, M.; Rega, N.; Millam, N. J.; Klene, M.; Knox, J. E.; Cross, J. B.; Bakken, V.; Adamo, C.; Jaramillo, J.; Gomperts, R.; Stratmann, R. E.; Yazyev, O.; Austin, A. J.; Cammi, R.; Pomelli, C.; Ochterski, J. W.; Martin, R. L.; Morokuma, K.; Zakrzewski, V. G.; Voth, G. A.; Salvador, P.; Dannenberg, J. J.; Dapprich, S.; Daniels, A. D.; Farkas, Ö.; Foresman, J. B.; Ortiz, J. V.; Cioslowski, J.; Fox, D. J. Gaussian, Inc., Wallingford, CT, 2009.
(25) (a) Becke, A. D. *J. Chem. Phys.* **1993**, *98*, 5648−5652. (b) Lee, C.; Yang, W.; Parr, R. G. *Phys. Rev. B* **1988**, *37*, 785−789. (c) Stephens, P. J.; Devlin, F. J.; Chabalowski, C. F.; Frisch, M. J. *J. Phys. Chem.* **1994**, *98*, 11623−11627.
(26) B3LYP level calculations showed that the examined reaction is endothermic. It has been pointed out that DFT calculations using B3LYP functional underestimate the reaction energies for conjugate additions.[27] Then, we also carried out M06/6-31G**//B3LYP/6-31G* level calculations, and the results showed that our qualitative discussion remains unchanged although the reaction is exothermic. See the Supporting Information.
(27) Rokob, T. A.; Hamza, A.; Pápai, I. *Org. Lett.* **2007**, *9*, 4279−4282.
(28) The computational details, including the energy profile, are described in the Supporting Information.
(29) The binary-complex models described in this paper would predetermine the preference of the reaction mechanism via the ternary complex B by the linkage. Therefore, as a model of the ternary complex A, we also investigated the reactions of the electrophiles **25** and **26** with nucleophiles such as nitromethane. However, no acceleration was observed in the reaction, and only a trace amount of adduct was obtained. This preliminary result would also make the ternary complex B more reliable.

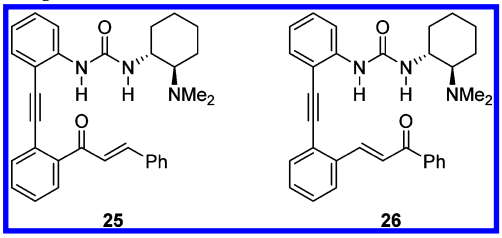

(30) Lin, C.-I.; Selvi, S.; Fang, J.-M.; Chou, P.-T.; Lai, C.-H.; Cheng, Y.-M. *J. Org. Chem.* **2007**, *72*, 3537−3542.
(31) Chow, K.; Corpuz, E.; Garst, M. E.; Heidelbaugh, T. M.; Nguyen, P. *J. Org. Chem.* **2003**, *68*, 10195−10198.